การดัดแปรผิวของควอนตัมดอต CdSe-ZnS ด้วยฟอสโฟลิพิดจากชาน้ำมัน *Camellia oleifera* Abel.

นายศราวุธ แผ่นทอง

วิทยานิพนธ์นี้เป็นส่วนหนึ่งของการศึกษาตามหลักสูตรปริญญาวิทยาศาสตรมหาบัณฑิต
สาขาวิชาเทคโนโลยีชีวภาพ
คณะวิทยาศาสตร์ จุฬาลงกรณ์มหาวิทยาลัย
ปีการศึกษา 2558

SURFACE MODIFICATION OF CdSe-ZnS QUANTUM DOTS WITH PHOSPHOLIPID FROM OIL-SEED CAMELLIA *Camellia oleifera* Abel.

Mr. Sarawuth Phaenthong

A Thesis Submitted in Partial Fulfillment of the Requirements
for the Degree of Master of Science Program in Biotechnology
Faculty of Science
Chulalongkorn University
Academic Year 2015

Thesis Title	SURFACE MODIFICATION OF CdSe-ZnS QUANTUM DOTS WITH PHOSPHOLIPID FROM OIL-SEED CAMELLIA *Camellia oleifera* Abel.
By	Mr. Sarawuth Phaenthong
Field of Study	Biotechnology
Thesis Advisor	Numpon Insin, Ph.D.

Accepted by the Faculty of Science, Chulalongkorn University in Partial Fulfillment of the Requirements for the Master's Degree

.....Dean of the Faculty of Science
(Associate Professor Polkit Sangvanich, Ph.D.)

THESIS COMMITTEE

.....Chairman
(Associate Professor Vudhichai Parasuk, Ph.D.)

.....Thesis Advisor
(Numpon Insin, Ph.D.)

.....Examiner
(Associate Professor Supason Wanichwecharungruang, Ph.D.)

.....External Examiner
(Nisanart Charoenlap, Ph.D.)

ศราวุธ แผ่นทอง : การดัดแปรผิวของควอนตัมดอต CdSe-ZnS ด้วยฟอสโฟลิพิดจากชาน้ำมัน *Camellia oleifera* Abel. (SURFACE MODIFICATION OF CdSe-ZnS QUANTUM DOTS WITH PHOSPHOLIPID FROM OIL-SEED CAMELLIA *Camellia oleifera* Abel.) อ.ที่ปรึกษาวิทยานิพนธ์หลัก: นำพล อินสิน, 81 หน้า.

ในงานวิจัยฉบับนี้ ทำการเตรียมควอนตัมดอต CdSe-ZnS ที่มีความสามารถในการกระจายตัวในน้ำได้ โดยการใช้สารฟอสฟอลิปิดที่ได้จากธรรมชาติในการดัดแปรผิว รวมทั้งศึกษาความเสถียรและความเป็นพิษต่อเซลล์ของอนุภาคดังกล่าว ทำการสกัดสารกลุ่มฟอสฟอลิปิดจากชาน้ำมัน สายพันธุ์ *Camellia oleifera* Abel.โดยกระบวนการ degumming ด้วยกรด 85% ฟอสโฟริก พบว่ามีปริมาณร้อยละผลได้ (percent yield) เท่ากับ 1.69% ต่อน้ำหนักของน้ำมันชาเริ่มต้น จากนั้นตรวจสอบความบริสุทธิ์และโครงสร้างโดยใช้เทคนิคฟูเรียร์ทรานฟอร์มอินฟราเรด สเปกโตรสโคปี (FT-IR), โปรตอนนิวเคลียร์แมกเนติกเรโซแนนซ์ สเปกโตรสโคปี (^{1}H-NMR) และฟอสฟอรัสนิวเคลียร์แมกเนติกเรโซแนนซ์ สเปกโตรสโคปี (^{31}P-NMR) พบว่า ฟอสโฟลิปิดที่ได้มีหมู่ฟังก์ชั่นได้แก่ C-H bonding, หมู่ คารบอนิล (C=O), and หมู่ฟอสเฟส (PO_2) โดยลักษณะสูตรโครงสร้างที่ได้คล้ายคลึงกับสายโซ่ในไตรกลีเซอไรด์ (triglyceride) ในน้ำมันชา และสารกลุ่มฟอสโฟลิปิดที่ได้จากชาน้ำมันประกอบด้วย ฟอสโฟลิปิดประเภท phosphatidylcholine และ lysophosphatidylethanolamine จากนั้นทำการสังเคราะห์ควอนตัมดอตประเภท CdSe-ZnS ขนาดต่างๆกันโดยใช้เทคนิค Hot rapid injection ผลพบว่า ได้อนุภาคควอนตัมดอตที่เปล่งแสงสีเขียว สีส้ม และสีแดง ที่มีขนาดเส้นผ่านศูนย์กลาง เท่ากับ 2.67 นาโนเมตร, 3.34 นาโนเมตร และ 4.48 นาโนเมตร โดยมีเปอร์เซ็นต์ quantum yield สูงโดยมีค่าเท่ากับ 33.44%, 24.9% และ 33.36% โดยมีความยาวคลื่นของแสงฟลูออเรสเซนต์ที่เปล่งออกมา มีค่าเท่ากับ 560, 578, และ 628 นาโนเมตร ตามลำดับ หลังจากนั้นนำสารกลุ่มฟอสโฟลิปิดที่สกัดได้ มาดัดแปรผิวด้วยวิธีการสร้างไมเซลล์ล้อมรอบอนุภาคเดิมพบว่าควอนตัมดอตหลังการถูกดัดแปรผิวด้วยสารฟอสโฟลิปิดทั้งสามขนาด พบว่าควอนตัมดอตสีเขียว, ควอนตัมดอตสีส้ม และควอนตัมดอตสีแดงหลังถูกดัดแปรผิวมีเปอร์เซ็นต์ quantum yield เท่ากับ 2.84%, 1.30% และ 2.43% โดยมีความยาวคลื่นของแสงฟลูออเรสเซนต์ที่เข้มสูงสุด มีค่าเท่ากับ 566, 585, และ 631 นาโนเมตร ตามลำดับ รวมทั้งไม่พบการเปลี่ยนแปลงของกราฟการดูดซึมแสงของควอนตัมดอต มีการลดลงของสัญญาณฟลูออเรสเซนต์และขนาด และไม่พบการเปลี่ยนแปลงรูปร่างของควอนตัมดอตและควอนตัมดอตที่ถูกแปรผิวด้วยสารฟอสโฟลิปิดทั้งสามขนาดสามารถกระจายตัวในน้ำและยังคงความเสถียรในตัวทำละลายมีขั้วได้ดีกว่าเมื่อเทียบกับควอนตัมดอตเริ่มต้นที่ยังไม่ถูกการดัดแปรผิว นอกจากนี้ได้นำควอนตัมดอตที่ถูกดัดแปรผิวด้วยสารฟอสโฟลิปิดไปทดสอบความเป็นพิษต่อเซลล์ในห้องปฏิบัติการ (In vitro) พบว่าควอนตัมดอตที่ถูกแปรผิวด้วยสารฟอสโฟลิปิดมีค่าการอยู่รอดของเซลล์ที่สูงกว่าควอนตัมดอตที่ยังไม่ถูกดัดแปรผิวด้วยสารฟอสโฟลิปิดที่ความเข้มข้นสูงสุด 1 mg/mL และจากการตรวจวัดการหลั่งสารไซโตไคน์ TNF-α, IL-6, และ IL-1β ของเซลล์ RAW 264.7 Macrophage เมื่อบ่มกับควอนตัมดอตที่ไม่ถูกดัดแปรผิวและควอนตัมดอตที่ถูกดัดแปรผิวด้วยสารฟอสโฟลิปิดเป็นเวลา 24 ชั่วโมงผลพบว่า สามารถตรวจพบการหลั่งของไซโตไคน์ TNF-α และ IL-6 ได้ แต่ไม่ตรวจพบการหลั่งของไซโตไคน์ IL-1β จากงานวิจัยนี้สรุปได้ว่าสามารถนำฟอสโฟลิปิดที่เป็นผลพลอยได้จากกระบวนการปรับปรุงคุณภาพของน้ำมัน มาใช้ประโยชน์ในการเป็นสารที่ใช้ในการดัดแปรผิวของควอนตัมดอตให้มีความสามารถในการละลายน้ำได้ เพื่อลดการใช้สารเคมีที่เป็นพิษและยังลดความเป็นพิษของควอนตัมดอต ควอนตัมดอทที่ได้มีศักยภาพในการพัฒนาใช้งานในด้านชีววิทยาโดยเป็นวัสดุทางเลือกใหม่ในการให้แสงฟลูออเรสเซนส์ในการตรวจวัดได้

สาขาวิชา เทคโนโลยีชีวภาพ ลายมือชื่อนิสิต .....

ปีการศึกษา 2558 ลายมือชื่อ อ.ที่ปรึกษาหลัก .....

5572121023 : MAJOR BIOTECHNOLOGY

KEYWORDS: QUANTUM DOT, EXTRA VIRGIN CAMELLIA OIL, PHOSPHOLIPID, DEGUMMING PROCESS

SARAWUTH PHAENTHONG: SURFACE MODIFICATION OF CdSe-ZnS QUANTUM DOTS WITH PHOSPHOLIPID FROM OIL-SEED CAMELLIA *Camellia oleifera* Abel.. ADVISOR: NUMPON INSIN, Ph.D., 81 pp.

In this work, we studied the preparation of water-dispersible fluorescent CdSe-ZnS core-shell quantum dots (QDs) using the surface modification with natural amphiphilic phospholipids (PLs) and investigated the stability and cytotoxicity of the results QDs. We isolated the amphiphilic phospholipids from extra virgin camellia (*Camellia oleifera* Abel.) oil by degumming process using acid treatment with 85% phosphoric acid. The results showed that the highest percent yield of the camellia phospholipids was 1.69% w/w of total extra virgin of camellia oil. The functional groups of camellia phospholipids comprised C-H bonding, carbonyl group(C=O), and PO_2 as characterized by Fourier transform infrared spectroscopy, Proton nuclear magnetic resonance spectroscopy (^{1}H-NMR) and 31-Phosphorus Nuclear magnetic resonance spectroscopy (^{31}P-NMR). The structures of camellia phospholipids were similar to the corresponding triglyceride and mainly comprised the phosphatidylcholine and lysophosphatidylethanolamine. Furthermore, we synthesized the trioctylphophine oxide-coated CdSe-ZnS QDs (TOPO-CdSe-ZnS QDs) of different sizes by hot rapid injection including green-emitting QDs (2.67 nm), orange-emitting QDs (3.34 nm) and red-emitting QDs (4.48 nm) Before modification, the original TOPO-CdSe-ZnS QDs in hexane exhibited high quantum yield of 33.44% for green QDs, 24.9% for orange QDs and 33.36% for red QDs with the highest emission wavelength at 560, 578, and 628 nm, respectively. Then, the original QDs of different sizes were modified with camellia phospholipids through micelle formation. After modification with camellia phospholipids, the PLs-coated CdSe-ZnS QDs in 1 M Tris pH 10 exhibited the quantum yield of 2.84% for PLs-green QDs, 1.30% for PLs-orange QDs, and 2.43% for PLs-red QDs with the maximum emission peaks at 566 nm, 585 nm, and 631 nm, respectively. Moreover, The PLs-coated CdSe-ZnS QDs of three sizes in media retained the absorption spectra and unchanged in shapes, and the PLs-coated CdSe-ZnS QDs were dispersible and stable in aqueous media when compared with the TOPO-CdSe-ZnS QDs. For cytotoxicity test, the PLs-coated CdSe-ZnS QDs showed higher cell viability than the original TOPO-CdSe-ZnS QDs at high concentrations of 1mg/ml. For cytokine detection, the original TOPO-CdSe-ZnS QDs and the PLs-coated CdSe-ZnS QDs of three sizes induce the release in TNF-α and IL-6, but not IL-1β after 24 h incubation in 264.7 raw cell. From the results, we could use the byproducts from plant edible oil production such as phospholipids in the preparation of water-dispersible quantum dots, leading to reduction in toxic chemicals used and QDs with low toxicity in vitro. The obtained water-dispersible quantum dots were potentially useful for biological applications as alternative fluorescent markers and sensors.

Field of Study: Biotechnology Student's Signature .....

Academic Year: 2015 Advisor's Signature .....

ACKNOWLEDGEMENTS

Firstly, I would like to appreciate Dr. Numpon Insin who is my thesis advisor, gave me valuable assistance to achieve my thesis successfully complete. Moreover, I would special thank Dr. Patcharee Ritprajak for laboratory supporting about cytotoxicity experiments.

For valuable comment and advices, I would like to thank my thesis committee, Associate Professor Dr. Vudhichai Parasuk, Associate Professor Dr. Supason Wanichwecharungruang and Dr. Nisanart Charoenlap. The research would have not been complete without all of their kidness.

In addition, I would like to thank all of members of Materials Chemistry and Catalyst Research Unit who are always helpful. Especially, Miss Wishulada Injumpa, Miss Chalatan Saengruengrit, Miss Padtaraporn Chunhom, Mr. Korakot Niyomsat and Mr. Phranot Ajkidkarn.

Other special group is my family who gave me everything for my life and furthermore, they are my encouragement for working on this research.

Finally, I would like to thank The Tea Oil and Plant Oils Development Center, Chaipattana Foundation, Mae Sai District, Chiang Rai Province for material supporting.This work was partly funded by the Thailand Research Fund, the Grants for Development of New Faculty Staff, and the 90th Anniversary of Chulalongkorn University, Rachadapisek Sompote Fund. Additionally, we would like to thank Program in Biotechnology, Department of Chemistry, Faculty of Science and Chulalongkorn University for laboratory faculties and instruments.

CONTENTS

Page

Page

Page

Page

Page

LIST OF FIGURES

LIST OF TABLES

LIST OF ABBREVIATIONS

QDs	=	Quantum dots
PLs	=	Phospholipids
Original TOPO-CdSe-ZnS QDs or pure QDs	=	Original CdSe-ZnS quantum dots passivated with triocylphosphine oxide and dissolved in hexane.
PLs-coated CdSe-ZnS QDs	=	CdSe-ZnS quantum dots modified with camellia phospholipids and dissolved in aqueous media.
mPAA-coated CdSe-ZnS QDs	=	CdSe-ZnS quantum dots modified with modified poly(acrylic acid) and dissolved in aqueous media.
mL	=	Milliliter
µL	=	Microliter
h	=	Hour
min	=	Minute
g	=	Gram
mg	=	Milligram

CHAPTER I
INTRODUCTION

1.1 Statement of the problem

Nanotechnology is a technology that emerged from the studies of materials with very small sizes called nanomaterials and their properties leading to applications in various fields. Quantum dots (QDs) are semiconductor nanocrystals with the particle sizes of about 2- 10 nm. The properties of QDs are unique and different from their bulk counterparts such as tunable fluorescent wavelength by controlling size, broad excitation spectra, more photo stability and giving high quantum yield of fluorescence. Recently, QDs have been successfully used as tools for fluorescence imaging of cancer cells, in vivo imaging, and protein sensor etc.

In typical preparations, as-synthesized original QDs were low dispersed in water or aqueous solvents because the original stabilizing ligands are Triocylphosphine (TOP) and Triocylphosphine oxide (TOPO) which hydrophobic properties. Therefore, the original hydrophobic surfactant layer of the original QDs should be replaced with hydrophilic or amphiphilic ligands for increasing the dispersity of QDs in aqueous media. Recently, many research groups synthesized the amphiphilic ligands that could substitute the original hydrophobic ligands, resulting in aqueous QDs. However, the synthesis processes of these ligands are usually complex and require a lot of chemicals, some of which are too toxic to be used in some applications and to be exposed to environment. For these reasons, we are interested in using natural amphiphilic ligands such as plant phospholipids as an alternative ligands for QDs. The phospholipid molecules are amphiphilic molecules that consist of two chains of steric aliphatic hydrocarbon and one of glycerol phosphatides as hydrophilic and hydrophobic parts, respectively. Normally, the plant phospholipids were by-products of refining oil process in plant oil industry.

In this research, the plant phospholipids were extracted from extra virgin tea oil from *Camellia oleifera* Abel. by mimicking the degumming process of crude plant oil, in which the gums were precipitated using phosphoric acid. The original QDs

synthesized by hot injection method into high boiling point organic solvents that contained capping ligands such as TOP and TOPO, were reduced their hydrophobicity by replacing the original ligands with the amphiphilic plant phospholipids. The obtained QDs in aqueous solutions will be studied for their potential in biological applications.

1.2 Objective of this research

The purposes of this study are:

1. To extract, characterize and identify the phospholipid compounds from *Camellia oleifera* Abel.
2. To modify the surface of quantum dots with phospholipid from *Camellia oleifera* Abel to increase the stability and dispersibility of QDs in aqueous conditions.

1.3 Expected benefits

The expected benefits of this study are that the quantum dots that are modified with natural phospholipid can disperse and yield long term fluorescent intensity in aqueous solutions. The QDs with lower toxicity could be applied in biological technology.

1.4 Scope of the thesis

Firstly, we synthesized quantum dots via hot injection methods and characterized using UV-Vis spectrometer and fluorescent spectrophotometer. Next, we extracted phospholipids from extra virgin Camellia oil that was obtained from The Tea Oil and Plant Oils Development Center, Chaipattana Foundation, Mae Sai District, Chiang Rai and pure cold pressed camellia oil (*Camellia olerifera* Abel.) from the Aromatherapy Shop Ltd., Somerest, TA3 7QB, UK. The functional group of Camellia phospholipids were characterized using Fourier transform infrared spectra (FT-IR), and the structures of Camellia phospholipids were analyzed using Proton nuclear magnetic resonance (^{1}H-NMR) spectroscopy and 31-Phosphorus nuclear magnetic resonance spectroscopy (^{31}P-NMR). Then, we modified the surface of QDs that were originally soluble only in non-aqueous solution to become dispersible in aqueous phase using

camellia phospholipids. The unmodified QDs and modified QDs were characterized by UV-Vis spectrophotometer, fluorescent spectrometer and calculated for the quantum yield. The unmodified QDs and modified QDs were measured the particle size and shape using transmission electron microscopy (TEM). Finally, the modified QDs were tested for their stability in aqueous media and cell toxicity *in vitro* in comparison with the unmodified quantum dots.

CHAPTER II

THOERY AND LITERATURE REVIEWS

2.1 Theories

2.1.1 Nanomaterials

Nanomaterials are materials that are of nanometer size in dimension lower than 100 nm.[1] The structures of nanomaterials can be classified by modulating dimensionalities. Zero dimensional (0D) materials are ones with all three dimensions falling in nanoscale. Some researchers called the 0D nanomaterial structures as nanoparticles, semiconductor nanocrystal quantum dots (QDs), nanosphere, etc. For the second types, one dimensional (1D) materials have two dimensions falling in nano-scale and another one is falling out of nano-scale. 1D nanomaterials include nanotubes, nanowires and nanorods. In contrast, two dimensional materials (2D) have two dimensions out of nano-scale range. Examples of 2D nanomaterials include thin films, nanolayers and nanosheets. Three dimensional materials (3D) are called bulk materials because all dimensions are falling into macroscale range, or no dimensions are dropping into nanoscale. Bulk materials can be developed to exhibit high surface area and possess many absorption sites for attaching molecules and can be applied in various applications such as catalysts, electrodes, materials for batteries, etc.[2] Images of examples of nanomaterials were shown in Figure 2.1.

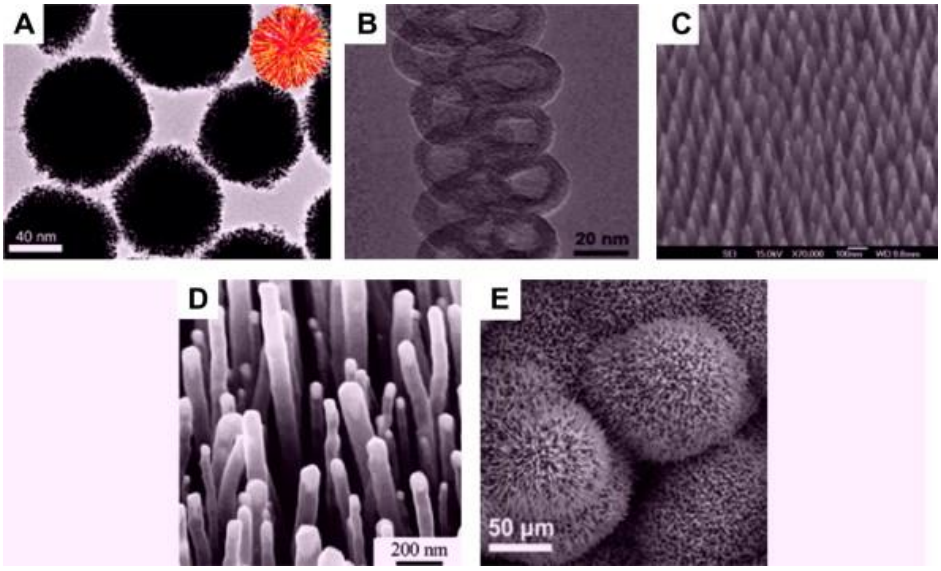

Figure 2.1: TEM and SEM images of examples of nanomaterials including (A) Nanoballs (dendritic structure) , (B) nanocoils, (C) nanocones, (D) nanopillers and (E) nanoflowers.[3]

There are two factors that promote the unique properties of nanomaterials. The two factors are high surface area to volume ratio and quantum confinement. When the given materials were broken down from a larger piece into smaller pieces, the surface area increases at given the volume. This phenomenon results in materials with more chemically reactive. For quantum confinement, when large materials are broken to smaller material in nanoscale as nanomaterials, the electronic energy levels become discrete (finite density of states), because of the confinement of the electronic wave function to the physical dimensions of the particles.[4] The unique properties of nanomaterial include electrical, optical, mechanical and magnetic properties. Examples of nanomaterials that display unique properties include metallic nanoparticles, magnetic nanoparticles and semiconductor nanoparticles.

2.1.2 Metallic nanoparticles

Metallic nanoparticles, especially gold (Au) and silver (Ag) nanoparticles, have been used to apply in various scientific fields. Gold and silver nanoparticles have long history in science, as well as esthetic and medicinal purposes. For example, the Egyptian used the gold nanoparticles in dentistry. In present day, the Au and Ag nanomaterials have increasingly developed to apply in biomedical fields and engineering fields due to their colloidal stability, unique properties and less cytotoxicity compared to other metal in nanoscale.[5]

2.1.2.1 Gold nanoparticles

Gold nanoparticles are colloidal suspension of gold that its particle sizes are about 10-20 nm. The suspension of gold nanoparticles is observed in red to purple color as its optical properties depend on the particle sizes. The different of color suspension of gold nanoparticles in various pH was shown in Figure 2.2. In early history, the gold nanoparticles were used to stain glasses for decoration. Recently, scientists

used the optical properties of gold nanoparticles to widely apply in various technology such as biological imaging, electronic devices and material sciences.

Figure 2.2: The solutions of Au nanoparticles in various pH (A) 1.97, (B) 3.16, (C) 5.13, (D) 6.64, (E) 8.08, (F) 10.57, (G) 10.77, (H) 11.12, and (I) 11.63.[6]

2.1.2.2 Silver nanoparticles

Silver nanoparticles (Ag-NPs) are colloidal suspension of silver that their particle size are about 1-100 nm. Ag-NPs were used to stain glasses for decoration similar to gold nanoparticles for decades. In present time, it have been established that Ag-NPs have unique biological properties, chemical properties, and physical properties when compared their bulk materials. Furthermore, the nanoparticles have particular physico-chemical properties, including a high electrical thermal conductivity, chemical stability, and catalytic activity. Therefore, recently, scientists have been developed the Ag-NPs to use in various applications including consumer products, disinfecting medical devices, environment treatment, electronics and computers application, etc. The Figure 2.3 showed the suspension of Ag-NPs in different sizes.[5]

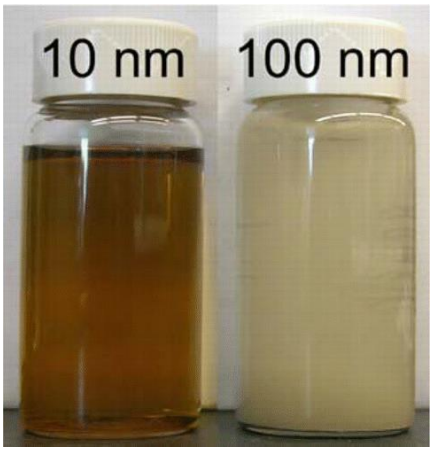

Figure 2.3: The photograph of silver nanoparticles in different sizes such as 10 nm for small size (left) and 100 nm for large size (right).[7]

2.1.3 Magnetic nanoparticles

The magnetic nanoparticles comprises ferromagnetic or ferrimagnetic materials such as iron and magnetite iron oxides. The unique properties of magnetic nanoparticle are superparamagnetic or strong magnetic response under magnetic fields. Recently, researchers used the properties to encourage the transport of therapeutic agents to specific targets for therapy and other applications. However, the outer surface of magnetic nanoparticle should be modified with biocompatible and non-toxicity coating before used in biological applications. Figure 2.4 illustrated the magnetic nanoparticle suspension when an external magnetic field was applied.[8]

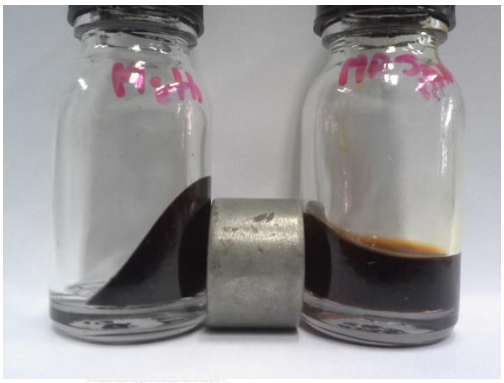

Figure 2.4: Magnetic nanoparticle dispersion when an external magnetic field from a strong magnet was applied.[9]

2.1.4 Semiconductor nanoparticles

Materials are classified into 3 types based on their electrical conductivities including conductors, semiconductors and insulators. In conductors, the conduction band and valence band are overlapped, or the valence band is not filled. For insulators, the band gaps between the conduction band and valence band are large. The electron from the valence band cannot be excited to the conduction band, resulting in no conductivity. For semiconductors, the electronic structures are the same as insulators, but the band gaps are smaller than that of the insulators as shown in Figure 2.5. In addition, when electrons are stimulated from the conduction band to valence band, fluorescent signal will be observed in some semiconductor materials. Semiconductor nanoparticles are conventionally called quantum dots (QDs).

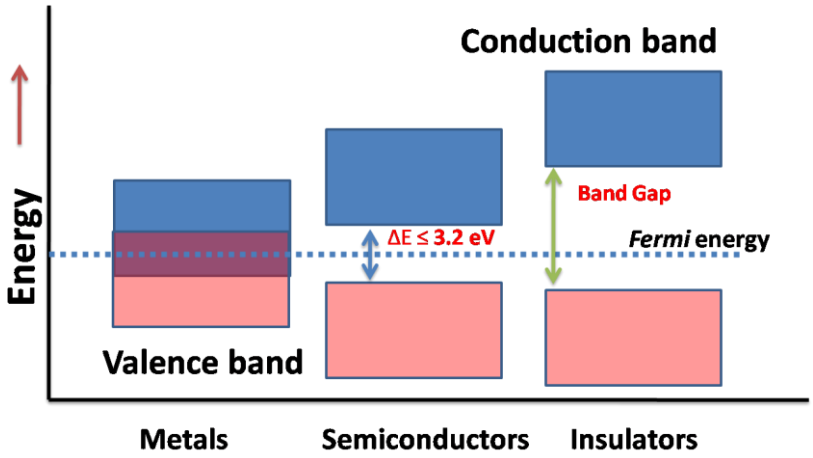

Figure 2.5: Energy band diagram of metals, semiconductors, and insulators.[10]

2.1.5 Semiconductor nanocrystal quantum dots (QDs)

Quantum dots are composed of inorganic semiconductors of about few hundred and few thousand atoms that normally surrounded by organic outer layers. In many cases, QDs are dispersed in organic solvent because they were stabilized with hydrophobic ligand. Normally, the sizes of QDs are about 2-10 nm. Most fluorescent QDs are made of semiconductor compounds in groups III-V and II-VI in periodic table. Fluorescence in QDs can be explained using energy band of semiconductor as followed. Electron from the valence band is excited to conduction band by photon activation, resulting in the electron in unstable state. Electron will relax back into the hole of valence band again, and give some energy in form of photon emission or fluorescence. Fluorescence from QDs have a specific wavelength depending on the types and sizes of QDs as shown in Figure2.6[11], resulting in the unique properties of QDs of broad excitation and emission of the specific wavelength. The absorption, emission and the size-tunable luminescence properties of the six sizes of CdSe QDs were shown in Figure 2.7. In the same type of QDs photons are high in emission frequency or short wavelength when the particles are small. The other properties of QDs are high quantum yield of fluorescence and more stable than other organic fluorescent dyes.[12]

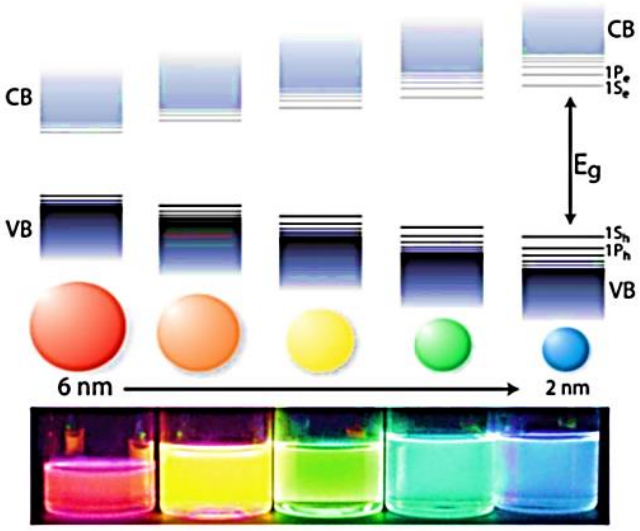

Figure 2.6: The quantum confinement effects: the band gap of the semiconductor material increases with decreasing size, and discrete energy levels arise at the band-edges.[13]

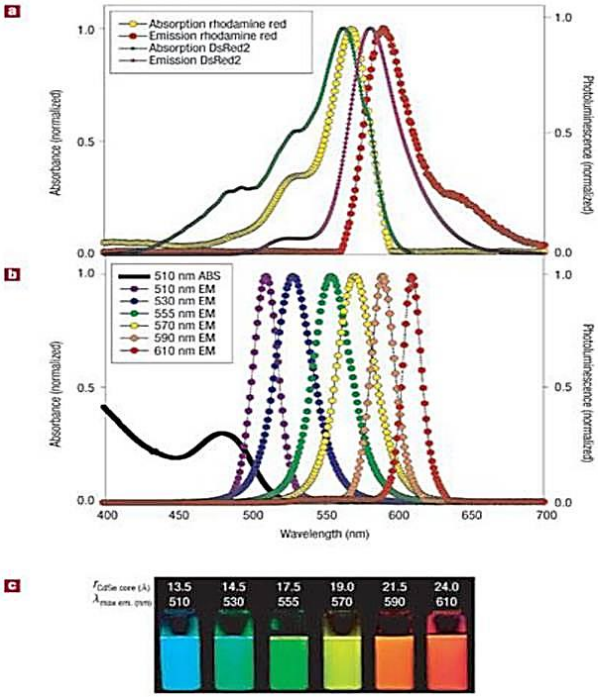

Figure 2.7: Absorption (a), emission (b), and the size-tunable luminescence properties and spectral range of the six sizes of CdSe QDs (c).[14]

2.1.6 Quantum dots synthesis techniques

The process of QD syntheses were generally aiming at controlling the sizes, homogenize, and surface coating of the resulted QDs. At present, the syntheses of QDs can be divided into 3 categories.

1. Hot injection into organometallic precursor
2. Low temperature reaction for aqueous QDs synthesis
3. Biosynthesis of QDs

In this research, we focus on the synthesis of CdSe QDs by hot injection of organometallic precursors. The method composes of three components including precursors, organic surfactants, and solvents. The precursors are composed of Cd^{2+} and Se precursors with trioctylphosphine (TOP) as a stabilizing ligand. The precursors were rapidly injected into boiling point of organic surfactant as trioctylphosphine oxide (TOPO). The nuclei of CdSe are formed by nucleation. Then, the nanocrystals were formed by aggregation of nuclei. The sizes of CdSe depend on the growth temperature and time. The mechanism of nucleation and nanocrystals formation are described in Figure 2.8.

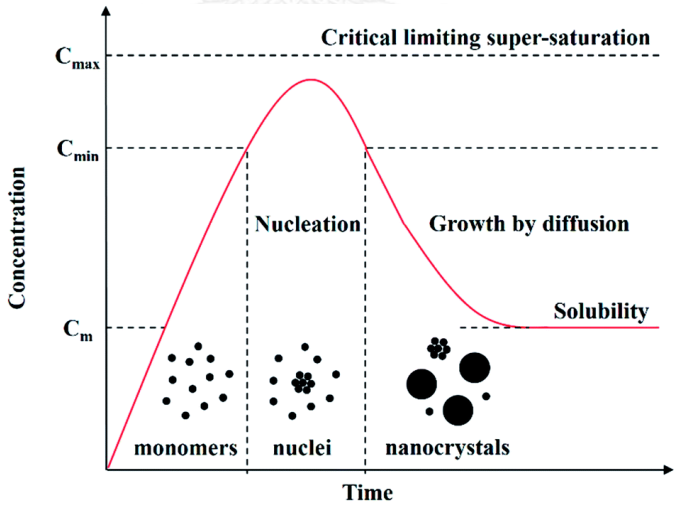

Figure 2.8: Schematic illustration of the nucleation and growth process of nanocrystals in solution: precursors are initially dissolved in solvents to form monomers, followed by the generation of nuclei and the growth of nanocrystals via the aggregation of nuclei.[15]

2.1.7 Structure of QDs for biological applications

In order to utilize QDs in biological applications, the QDs are usually modified to increase biocompatibility. The structures of QDs consist of three layers as shown in Figure 2.9.

For the innermost layer, the cores at the center of QDs are the key component that controls the optical properties of the nanoparticles. Typically, cores of QDs are composed of II–IV, IV–VI or III–V semiconductor (e.g. CdTe, CdSe, and CdS). In the second layer, the shells are coated around the cores. The shells are usually large band gap semiconductors such as ZnS, ZnSe, etc. This layer encourages the stability of QDs against the surface degradation. Generally, the original QDs are dispersed in such organic solvents as hexane. Thus, the original QDs have to be modified with hydrophilic ligands, such as polyethylene glycol (PEG), mercaptocarbonic acid, phospholipids, etc, on the outer layer in order to promote the biocompatibility.[16] The coating layers are important for use in biological applications.

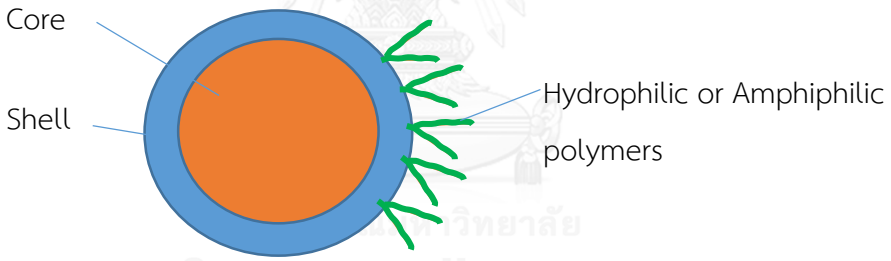

Figure 2.9: Structure of quantum dots for use in biological application including core (red), shell (blue), and modified ligand (green).

2.2 Phospholipids

Phospholipids are amphiphilic molecules that can be obtain from plants. We are interested in studying the potential of applying phospholipids as natural ligands for surface modifications of nanoparticles. In this section, structures, sources and modification processes of phospholipids are discussed in the following sections.

2.2.1 Structure of phospholipids

Phospholipids, a class of lipids, are main component of cell membrane in all living organisms. The structure of phospholipids consists of two steric aliphatic hydrocarbon chain as hydrophobic tails that might contain positive charges and

glycerol phosphatides (negative charge) as polar head groups. The general structure of phospholipids as shown in Figure2.10. The polar head groups compose of 'R' groups such as choline group: R = CH2CH2N+(CH3)3, that are character the each phospholipid species as shown in Table 2.1[17]

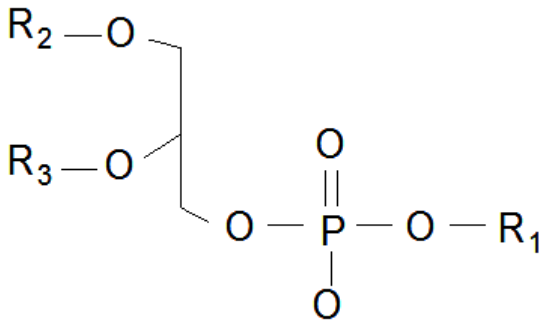

Figure 2.10: General structure of phospholipids.[18]

Phospholipid (R_1)	Hydrophobic chains (R_2,R_3) (name)	Lipid Name (Abbreviation)
Phosphatidylcholine $CH_2CH_2N^+(CH_3)_3$	$CH_3(CH_2)_7CH=CH(CH_2)_7C(O)$- (oleyl)	Dioleylphosphatidylcholine (DOPC)
	$CH_3(CH_2)_{12}C(O)$- (myristoyl)	Dimyristoylphosphatidylcholine (DMPC)
	$CH_3(CH_2)_{14}C(O)$- (palmitoyl)	Dipalmitoylphosphatidylcholine (DPPC)
	$CH_3(CH_2)_{16}C(O)$- (stearoyl)	Distearoylphosphatidylcholine (DSPC)
Phosphatidylethanolamine $CH_2CH_2NH_3^+$	$CH_3(CH_2)_7CH=CH(CH_2)_7C(O)$- (oleyl)	Dioleoylphosphatidylethanolamine (DOPE)
	$CH_3(CH_2)_{16}C(O)$- (stearoyl)	Distearoylphosphatidylethanolamir (DSPE)
Phosphatidylglycerol $CH_2CHOHCH_2OH$	$CH_3(CH_2)_{12}C(O)$- (myristoyl)	Dimyristoylphosphatidylglycerol (DMPG)
	$CH_3(CH_2)_{14}C(O)$- (palmitoyl)	Dipalmitoylphosphatidylglycerol (DPPG)
Phosphatidylserine $CH_2CHNH_3^+COO^-$	$CH_3(CH_2)_{14}C(O)$- (palmitoyl)	Dipalmitoylphosphatidylserine (DPPS)
	$CH_3(CH_2)_{16}C(O)$- (stearoyl)	Distearoylphosphatidylserine (DSPS)

Table 2.1: The differences in R1 R2 R3 groups in head region and hydrophobic chains of phospholipids for individual phospholipids species.[18]

Phospholipids are used as a good surfactants and emulsifiers. For example, lecithin is the phospholipid wildly used in commercial products. Originally, lecithin is extracted from egg yolk, and the main components are phosphoric acid with choline group as called phosphotidylcholine. At present, commercial lecithin can be easily

isolated from other various biological sources by chemical processes such as marine sources, modified crops, milk and especially, plants oil such as olive oil, sunflower oil, soybean and rapeseed oil.[19]

In this research, we extracted the phospholipids from extra virgin of tea oil camellia (*Camellia oileifera* Abel) which derived from the Chaipattana foundation, tea oil and plant oils development center, Mae Sai district, Chiang Rai province and pure cold pressed camellia oil (*Camellia olerifera* Abel.) from the Aromatherapy Shop Ltd., Willowbrook, Stapley, Churchstanton, Somerest, TA3 7QB, UK.

2.2.2 Tea oil camellia (*Camellia oleifera* Abel.)

Tea oil camellia (*Camellia oleifera* Abel.) is categorized in the Theaceae family, which was determined by Linnaeus (integrated Taxonomy Information System, 2006) as shown below:

Division Magnoliophyta
Class Magnoliopsida
Order Ericales
Family Theaceae
Genus Camellia
Species C. oleifara

Tea oil camellia is widely distributed in China. Commonly, the fatty acid compositions of camellia oil are oleic acid and linoleic acid. The two essential fatty acids are important for human consumptions because it can protect an accumulation of bad cholesterols in blood and maintain the nervous system and physiological functions. Moreover, camellia oil have many therapeutic agents that can be applied into lubricant and cosmetics.[20]

Figure 2.11: Tea seed camellia (*Camellia oleifera* Abel.).[21]

Figure 2.12: Virgin Camellia oil from tea oil and plant oils development center Chaipattana foundation.[22]

2.2.3 Refining process of edible oil.

Normally, edible oils are isolated from biological organisms such as plants oil, animals, algae, etc. Human used crude oil for consumption before the crude oil are upgraded from low quality into high quality because the crude oil is composes of various undesirable substances such as free fatty acid, pigments, waxes, heavy metals, odor and flavors.[23] The process of undesirable substances removal is called a refining

process. The process combines chemical processes and physical processes as shown in Figure 2.13.

The refining process includes four steps as followed.

1. **Degumming processes:** These steps are for eliminating the phosphatide residuals.
2. **Neutralizing or deacidification:** These steps are aiming at removing of free fatty acid by alkali neutralization, or chemical refining, and distillation, or physical refining.
3. **Bleaching:** Pigments are eliminated in bleaching steps.
4. **Deodorizing and stripping:** These steps are for removing odors in vacuum condition.

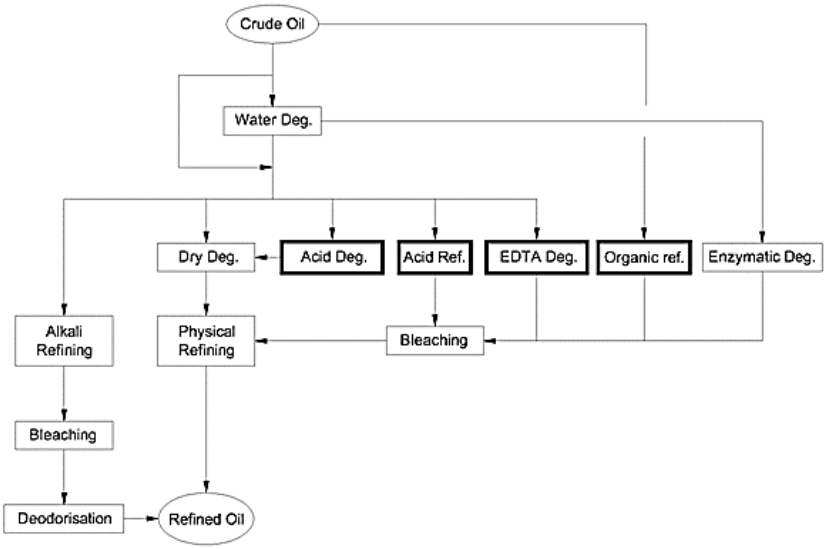

Figure 2.13: Overview of refining process which convert the crude oil into refined oil.[23]

2.2.3.1 Degumming process

The degumming process is of our focus in this research because phospholipids can be collected from this process. The degumming processes are for removing of the phosphatide substances and are the first step in refining oils. The degumming processes could be done in five methods.

1. Water degumming: Crude oils are treated by hot water to remove hydratable phosphatides.

2. Dry acid degumming: The crude oils are added by dry acid such as phosphoric acid, citric acid, oxalic acid, etc. The non-hydratable phosphatides, free fatty acid and some triglyceride are eliminated from crude oils.
3. Wet acid degumming: The process is similar to dry acid degumming but in the wet acid degumming, acids with small amount of water are used to increase hydration.
4. Special degumming: The process consists of the acid degumming with partial neutralization.
5. Enzymatic degumming: In this method, the phospholipids are modified with enzyme to obtain the water soluble compounds.[24]

In this work, the camellia phospholipids can be collected from by-products of dry acid degumming process with 85% phosphoric acid.

2.3 Surface modification of quantum dots

Surface modification is a process to change the properties of nanoparticle by coating or forming nanoparticles with ligands or polymer on their surfaces. In this research, the original QDs were stabilized with hydrophobic ligand (e.g. TOP, TOPO, etc.) on their surfaces. They could not dissolve in aqueous media, so they are toxic in environment, and non-biocompatibility. Therefore, the original QDs should be modified with hydrophilic or amphiphilic polymers before applied in biological system. Some biocompatible polymers can be coated on QD surfaces and protect them as a stable interface between QDs and biological networks, and decrease the toxicity.[25] Surface modification of QDs can be divided into two strategies including ligand exchange and encapsulation.

2.3.1 Ligand exchange

In the first strategy, the original ligands on nanomaterial surfaces are substituted with amphiphilic bifunctional ligands or polymers. The new ligands promote the dispersibility in aqueous solutions of nanomaterials. For example, Kimihiro used dihydrolipoic acid (DHLA) and polyethylene glycol (PEG) to exchange with the original ligand of CdSe-ZnS QDs for making the water-soluble QDs. In addition, the terminal of

ligands on outer layer could be coupled with biomolecules and applied in various fields.[26]

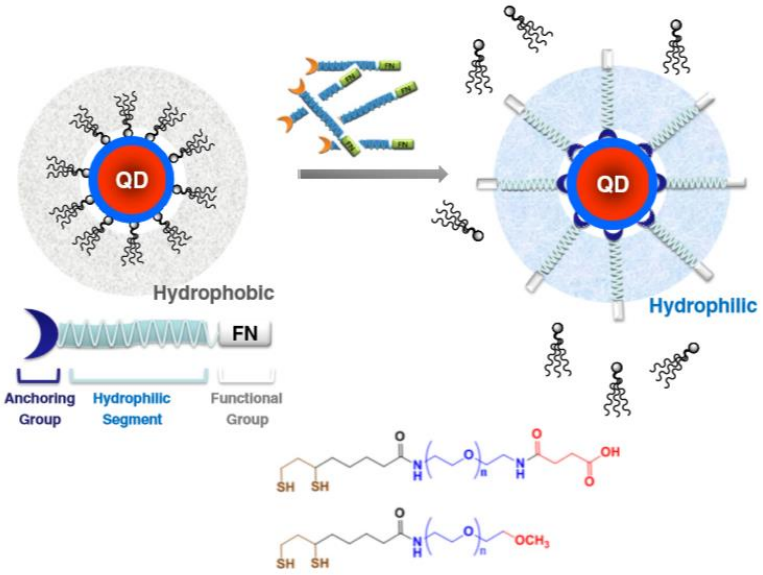

Figure 2.14: The substitution of hydrophilic ligands with hydrophilic ligands (DHLA-PEG-COOH) via ligand exchange.[27]

2.3.2 Encapsulation

For this strategy, the original surface are substituted with amphiphilic bifunctional ligands similar to ligand exchange, but the original ligands and the modifying ligand are both presented on the structures of the resulted nanomaterials. Mostly, bifunctional amphiphilic polymers contained some carboxylic groups and alkyl chain for controlling and balancing the hydrophobic and hydrophilic blocks within the polymer backbone. These phenomena could be used to stabilize the polymer coating on the original hydrophobic ligands and promote the water soluble of nanomaterials.[26] For example. Nathalie and coworkers synthesized the amphiphilic phospholipids that were derived from the ring opening metathesis of norbornene-based monomers to stabilize and solubilize the quantum dots by micelle formation used the scheme as shown in Figure 2.15.

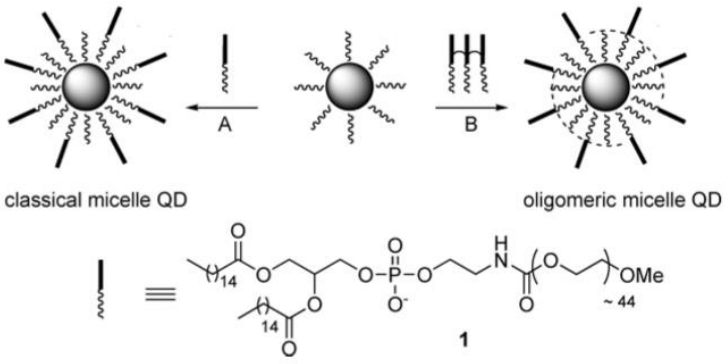

Figure 2.15: Schematic of modified QDs with synthesized phospholipids into classical micelle and oligomeric micelle QDs.[28]

In this research, we modified the surface of QDs with natural amphiphilic phospholipids from camellia oil by encapsulation using micelle formation.

2.4 Literature reviews

2.4.1 Camellia phospholipid

Lee C.P and Yen G.C in 2006 studied the antioxidant activity from bioactive compounds which was extracted from tea seed camellia oil with methanol. The bioactive compounds from tea seed oil included sesamin and a novel compound: 2,5-bis-benzo[1,3]dioxol-5-yl-tetrahydro-furo [3,4-d][1,3] dioxine, which were characterized by MS, IR, ^{1}H NMR, and ^{13}C NMR techniques. The results concluded that the two bioactive compounds from tea seed camellia oil promote antioxidant activity, and prevent free radical related diseases as prophylactic agents.[29]

In 2009, Fang Xue and co-worker extracted the high quality camellia oil and evaluated the indexes of the oil including acid value, peroxide value, β-carotene, polyphenols phospholipids and the content of vitamin E. In the comparison of processes used in the oil production, they compared three extraction methods including pressing, solvent extraction by n-hexane and aqueous enzymatic extraction. The aqueous enzymatic method yielded high acid value, content of vitamin E and β-carotene than other methods. On the other hand, the three extraction methods gave significant differences in the peroxide value. Total polyphenols and phospholipids content in the aqueous enzymatic method were 4.12 μg/g and 2.87 μg/g, which were different significantly from the other methods.[30]

The stereospecific positional distributions of fatty acid of camellia seed oil (*Camellia japonica*) was determined by silica gel column chromatography, thin layer chromatography and gas chromatography. They found that the camellia seed oil comprised of 88.2% of neutral lipid, 6.4% of glycolipids and 5.4% of phospholipids. The major of fatty acid composition in neutral lipid, glycolipid and phospholipid were oleic acid at 86.3%, 62.5% and 54.2%, respectively, and the minor of fatty acid were palmitic acid, stearic acids and linoleic acid. For positional distribution of camellia oil, oleic acid was distributed more at sn-2 positions (93.6%) and sn-3 positions (94.7%) than at sn-1 position (66.0%). (Siwon Noh and Suk Hoo Yoon, 2012).[31]

Occluded camellia oil and phospholipids (lecithin) production were recovered from wet soybean gums by water elimination and acetone extraction. Recovered oil contained about 588 g/kg of occluded oil when water was eliminated before extraction. In contrast, lecithin was not significantly obtainable from this method. Moreover, recovered oil had high oleic acid content and purified lecithin about 16.7–21.7 $g.kg^{-1}$, and 610-691 $g.kg^{-1}$of total phospholipids, respectively. The results suggested that the occluded oil in soybean wet gums can recover with high quality and stability. In addition, lecithin can be extracted and recovered with high purity. (Liliana N.C. and coworker, 2008)[32]

Wu Jing *et al*. studied about the degumming (removing gums) process from pressed tea seed oil using phosphoric acid and hydration methods. Furthermore, they studied the effects on degumming including degumming temperature, amount of phosphoric acid added, amount of water and degumming time. They concluded that the optimum conditions were degumming temperature of 50 °C, amount of 85% phosphoric acid of 0.2%, degumming time of 30 min and addition of 4% water of oil weight. The yield rate of degumming oil was 94%. The content of unsaturated fatty acid in tea seed oil reached 83% as characterized using GC-MS, and the linoleic content was about 25%.[33]

As reported by Lee and coworkers in 2014, they optimized the conditions of edible camellia oil during degumming, alkaline refining, bleaching, and deodorization processes. In degumming process, the phosphorus content in edible oil was eliminated from 57 ppm to 10 ppm using 85% phosphoric acid. The free fatty acid was removed

in alkaline refining step. In bleaching process, the Lovibind yellow were reduced from 11.0 to 1.1 when adding high concentration of activated clay. The peroxide values were slightly decreased when temperature increased, and the optimum bleaching time for acidified camellia oil was about 30 min. Also, the bleaching is process of reducing the edible oil color to reach final color specification of the refined products. In deodorization, the optimum of deodorization temperature was determined as 180 ºC. After processes, the edible oil was still high quality, high lipid components, which contain neutral lipids, phospholipids and glycolipids of 98.84 %, 1.03 %, and 0.13 %, respectively.[34]

Form literature reviews, camellia oil composed of many substances such as bioactive compounds, vitamin E, and polyphenol, especially phospholipids. The phospholipids are minor substances in camellia oil, and can be extracted by various methods including solvent extractions, aqueous enzymatic extractions, degumming processes etc. The degumming process using phosphoric acid could remove the phosphorus substances as byproducts from crude plant oil. Therefore, we are interested in employing the acid degumming process to extract the phospholipids from camellia oil using 85% phosphoric acid because the process could extract the phosphatide from plant oil even at low content, prevent the production of an aqueous effluent and cost lower price compared to other methods.[35]

2.4.2 Surface modification of QDs with amphiphilic polymers and applications

In 2010 Changhua et al. synthesized amphiphilic molecules such as polymaleic acid aliphatic alcohol ester amphiphilic oligomer (PMAA) and modified QDs of three different colors with the molecules to be transferrable from organic phase to aqueous phase. In biological conditions test, the modified QDs showed high consistency in the fluorescent intensity for 150 h at high temperature, and were highly stable in pH2 (0.01M) – pH14 (1M) solution for 3 h. From this study, it was shown that they were successfully modified the water insoluble QDs into the water soluble QDs with amphiphilic polymers, and the water soluble QDs can be applied for biological systems.[36]

Anupam and co-worker in 2012 determined the ligand exchange between the original TOPO capping of CdSe-ZnS QDs in toluene and L-arginine (Arg) amino acids in water. The results showed that the aqueous soluble Arg-capped QDs exhibited quantum yield of 14%. For application, they used their modified QDs (energy donor) with Ethidium labeled synthetic dodecamer DNA (energy acceptor) by a picosecond-resolved Forster resonance energy transfer (FRET) technique. The interaction between the Arg-capped QDs and DNA was hydrogen-bonding interaction with associative mechanism operating during the formation of QD-DNA nanobioconjugates. They suggested that amino acid-capped QDs conjugate with DNA may be improved to be useful in making FRET-based sensors.[37]

Jianbo Liu and co-worker in 2012 studied the microscopic structures and photo-physical properties of the phospholipid-quantum dot micelles. The two types of phospholipids included distearoylphosphatidylethanolamine (DSPE) and Poly (ethylene glycol)–distearoylphosphatidylethanolamine (PEG–DSPE). The surfactants were dispersed in chloroform, and QDs were added in. The mixtures were evaporated to remove the solvent and flushed with N2. The lipid film solution was hydrated with water at 80 ºC and ultra-sonicated for 10 min. PEG-DSPE-QDMs showed no obvious change the absorbance and fluorescent after encapsulation. In contrast, DSPE-QDMs spectrum showed a sloping baseline and slight quenching of fluorescent intensity due to DSPE-QDMs aggregation. In conclusion, DSPE was encapsulated with many QDs in one micelle. On the other hand, PEG–DSPE was encapsulated with only one QDs in single micelle.[38]

Yun Feng S. 2008, they presented the fabrication of phospholipids which were functionalized on the surface of CdSe-ZnS QDs by a partial exchange process as shown in Figure 2.16. The TOPO ligand was stabilized by S-H terminated phospholipid (PPLs). The PPL-functionalized QDs solution was translucent. After modification, the PPL-functionalized QDs showed weakening of S-H vibration and the CH2-S wagging vibration in CH2-SH structure, while the PO-CH2 rocking vibration in PO-CH2-structure was decreased. From TEM technique, the PPL-functionalized QDs were larger than non-functionalized QDs. The results may indicate that the PPL was functionalized on the QD surfaces, and the bilayer structure was formed on the QD surfaces.

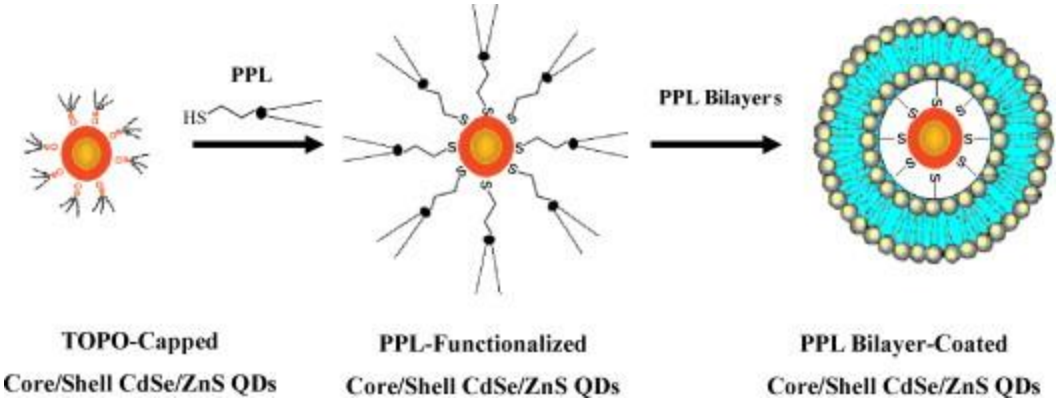

Figure 2.16: Preparation of PPL-functionalized core/shell CdSe-ZnS QDs.[39]

For applications of PPL-coated QDs, various biomedical researches have utilized the PPL-coated QDs. For example, the PPL-QDs were used in lineage-tracing embryogenesis experiments both in vitro and in vivo imaging as reported by Benoit in 2002. For in vitro, they encapsulated QDs with the phospholipid block copolymer into micellar forms as a fluorescent probe and hybridized with specific complementary DNA sequences. Then, for in vivo experiment, they injected the particles into Xenopus embryo as shown in Figure2.17. As a result, the PPL-QDs can perform as a stable, non-toxic, cell autonomous, and resistance to photo-bleach probe.

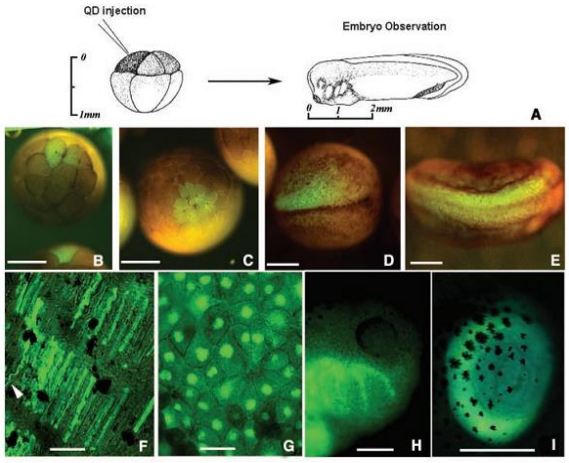

Figure 2.17: QD labeling of Xenopus embryos at different stages and specific QD intracellular localizations in in vivo experiment.[40]

The phospholipid-QD micelles were used in whole body imaging for quantifying the tumors in the near-infrared region as studied by Aristarchos P. in 2009. They

compared the whole body imaging between PEG-phospholipid micelle (QDs-M) and commercial PEGylated-QDs (QDs-PEG). The results were shown in Figure2.18. The QDs-M distributed both organs and tumors rapidly. Then, the fluorescent of QDs-M was clearly visible about 1-2 hours, which is comparable to QDs-PEG at half of QDs dose.

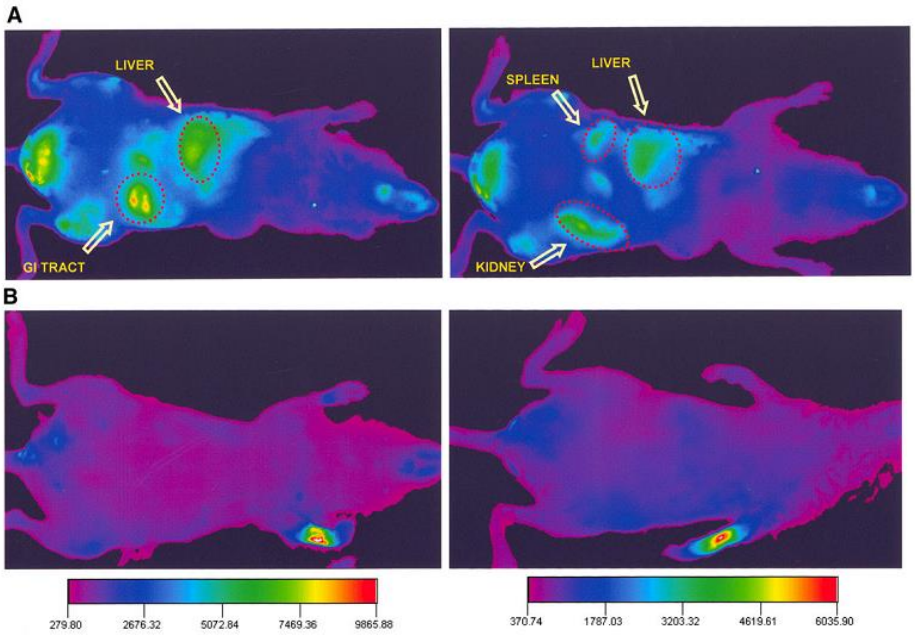

Figure 2.18: Whole-body images and color-coded map of mouse injected with QD-Ms (A) and QD-PEGs (B) (left at 1 hour; right at 2 hours).[40]

Bio-conjugated quantum dots were extensively developed to apply in biomedical research. Rui Hu and co-worker (2012) used near infrared emitting ultra-small lead sulfide (NIR-PbS) QDs. They encapsulated the NIR-PbS QDs with PEGylated phospholipids into PEGylated phospholipid micelles as shown in Figure2.19. The diglyceride groups of hydrophobic tails of phospholipids interacted with hydrophobic QDs into phospholipids –encapsulated QDs micelles. Then, they studied about cytotoxicity and applied in vitro and in vivo imaging.

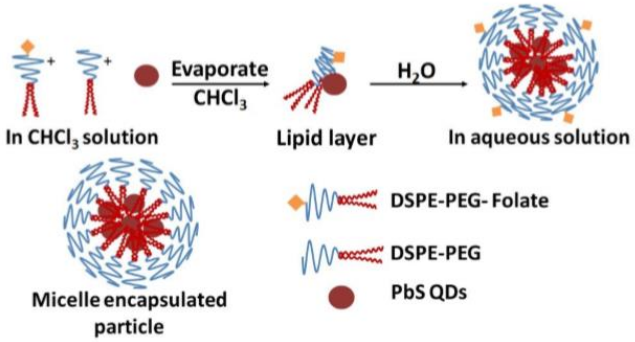

Figure 2.19: Preparation of encapsulated phospholipids PbS QD micelles.[41]

For cytotoxicity experiment, the toxicity of QDs was decreased when encapsulated with phospholipids micelles. For in vitro imaging, the folic acid functionalized micelle-encapsulated PbS QDs were up taken into the inner cellular of Human pancreatic cancer cell line more than the non-functionalized folic acid micelles encapsulated Pbs QDs. For in vivo imaging, the PEGylated phospholipid micelle encapsulated NIR PbS QDs formulation can be observed as an efficient high-contrast agent for small animal imaging. They concluded that the phospholipid encapsulated PbS QDs can be used to apply in the theranostic researches.

In 2013, Jing Liu and coworker studied the bio-parameters such as bio-distribution, animal weigh, hematology etc. The parameters were evaluated the effect of phospholipid micelles encapsulated CdSe/CdS/ZnS QDs on the long term in vivo toxicity in Kunming mice at an overdose (50 $mg.kg^{-1}$) for 16 weeks. The phospholipid micelles encapsulated CdSe/CdS/ZnS QDs were not toxic. Body weight and serum showed no change in any parameters in treated groups in mice. From histological study, all organs showed no acute toxicity effect *in vivo*. Moreover, QDs were nonspecific all take up in liver, spleen and lymph node, but QDs were not much accumulated in lung and kidney. In addition, the results supported that high stability of fluorescent QDs can be used as the therapeutic carriers due to the minimal health risk.[42]

From literature reviews, many researchers synthesized various amphiphilic ligands, including amphiphilic phospholipids, to modify onto the non-aqueous QDs into the aqueous QDs. Recently, some researchers are interested in the phospholipids molecules to prepare aqueous QDs for various applications, but the majority of their molecule prepared from animal tissue, plants or synthesis in chemical labs. In this research, we are also interested in the natural phospholipids that are by-products from degumming process of crude plant oils.

CHAPTER III

METHODOLOGY

In this research, we synthesized trioctylphosphine oxide-capped CdSe-ZnS quantum dots (TOPO-CdSe-ZnS QDs), and extracted the camellia phospholipids from extra virgin camellia oil by acid degumming process. Then, the original QDs were modified with camellia phospholipids by micelle formation. Stabilities and cytotoxicity of the resulted QDs were studied in order to determine the potential of using these QDs in biological applications.

The instruments and chemicals for synthesis of the original TOPO-CdSe-ZnS quantum dots are listed on Tables 3.1-3.2.

3.1 The instruments

Table 3.1: List of instruments

Characterization techniques	Models
Ultraviolet-visible spectroscopy (UV-Vis spectroscopy)	Cary 50 (Varian)
Fluorescent spectroscopy	Cary Eclipse (Varian)
Transmission electron microscope (TEM)	JEM-2100 (JOEl)
Dynamic light scattering analyzer (DLS)	Zetasizer nano ZSP (Malvern)
Gas chromatography (GC)	CP-3800 (Varian)
Fourier transform infrared spectroscopy (FT-IR)	Impact 410 (Nicolet)
Proton nuclear magnetic resonance (^{1}H-NMR)	Avance 400 (Bruker)
Phosphorus nuclear magnetic resonance (^{31}P-NMR)	Avance III HD (Bruker)

3.2 Materials and chemicals

Extra virgin Camellia tea oil was obtained from The Tea Oil and Plant Oils Development Center, Chaipattana Foundation, Mae Sai District, Chiang Rai Province, and pure cold-pressed camellia oil (*Camellia olerifera* Abel.) from the aromatherapy shop Ltd., Willowbrook, Stapley, Churchstanton, and Somerset, TA3 7QB, UK.

All chemicals in this research are listed on the Table 3.2.

Table 3.2: List of chemicals

Chemicals	Supplier
Trioctylphosphine oxide (TOPO), 90% technical grade	Aldrich, United States
Trioctylphosphine (TOP), 97%	Aldrich, United States
1-Hexadecylamine (HDA), 98%	Aldrich, United States
Zinc acetylacetonate, 99.95%	Aldrich, United States
Cadmium 2,4-pentanedionate ($Cd(acac)_2$), ≥99.9%	Aldrich, United States
1,2-hexadecanediol (HDDO), 90% technical grade	Aldrich, United States
Selenium powder, ≥99%	Riedel-de Haen, United States
Sulfur powder, ≥99.99%	Aldrich, United States
Triocylamine, 98%	Aldrich, United States
Hexane, AR grade	J.T. Baker, United States „
Ethanol, AR grade	Merck, Germany
Chloroform, AR grade	RCI Labscan, Thailand
Acetone, AR grade	RCI Labscan, Thailand
85% phosphoric acid, AR grade	RCI Labscan, Thailand
Trizma® base, ≥99.9%	Aldrich, United States

In this research, the experiments are divided into four steps.

1. Synthesis of quantum dots
2. Extraction of camellia phospholipids
3. Surface modification of original TOPO-CdSe-ZnS QDs with camellia phospholipids
4. Colloidal stability and cytotoxicity test

3.3 Synthesis of quantum dots

Semiconductor nanocrystal quantum dots were synthesized at boiling point of organic solvent which contained the original capping ligand such as Tri-octylphosphine oxide (TOPO), Tri-octylphosphine (TOP) and other surfactants by hot injection methods.[43] The process was composed of two steps including synthesis of CdSe core and coating the cores with ZnS shell.

3.3.1 Synthesis of CdSe core

3.3.1.1 Preparation of 1.5 M TOPSe

5.92 g of selenium powder (Se powder) in 125 mL Erlenmeyer flask was placed under vacuum for 30 min. Then, Se powder in flask was injected with 50 mL TOP under N_2 atmosphere, and the mixture was stirred overnight to obtain colorless clear solution.

3.3.1.2 Preparation of the Cd and Se precursors

0.76 g of Cadmium 2, 4-pentanedionate ($Cd(acac)_2$) and 1.71 g of 1,2-hexadecanediol (HDDO) in small vial were placed under vacuum for 30 min and injected with 4 mL of TOP under N_2 inert gas. Then, the mixtures were stirred at 100°C for 1 h. After cooled down, the mixture was injected with 6 mL of 1.5 M TOPSe. The mixture of precursors should not become solidified before injected into the coordinating solvents at high temperature to allow the complete reaction.

3.3.1.3 Preparation of CdSe core

5.75 g of 1-Hexadecylamine (HDA) and 6.25 g of TOPO in 100mL three-necked bottle were placed under vacuum for 30 min. Then, the coordinating solvents were injected with 3.4mL of TOP under inert condition, and the mixture was stirred for 2 h. The Cd and Se precursors was rapidly injected at 360 °C, and this temperature was held for at least 2 min. CdSe quantum dots were formed at this step. Finally, CdSe core mixture was injected with 10 mL hexane at 60 °C, and kept in amber vials in order to protect the QDs from light.

3.3.2 ZnS shell coating

CdSe cores, which were capped with the TOP/TOPO capping groups on outer surfaces, were low quantum yield due to incomplete surface passivation.[43] Therefore, CdSe cores should be coated with ZnS shell for increasing the quantum yield of the QDs and protecting the QDs from surface degradation.

3.3.2.1 Preparation of TOPS

0.0641 g of sulfur powder was placed under vacuum for 30 min before the container was filled with nitrogen. The powder was injected with 5 mL of TOP under

nitrogen at room temperature, and the mixture was stirred overnight before a colorless solution of triocylphosphine sulfur (TOPS) was obtained.

3.3.2.2 ZnS shell coating

0.21 g Zinc acetylacetonate in 100 mL three-necked bottle was placed under vacuum for 30 min. The Zn precursor was injected with 5 mL of trioctylamine under inert gas. Then, the precursor was injected with CdSe quantum dots dispersed in hexane at 60°C. The mixtures were removed of hexane using a vacuum pump. TOPS was injected drop by drop into the mixture at 150°C. The CdSe-ZnS QDs mixture was added with 20 mL hexane, and kept in dark for further use.

3.4 Extraction of camellia phospholipids

In this research, we obtained the extra virgin of camellia oil from The Tea Oil and Plant Oils Development Center, Chaipattana Foundation, Mae Sai District, Chiang Rai Province, and pure cold pressed camellia oil (*Camellia olerifera* Abel.) from the aromatherapy shop Ltd., Willowbrook, Stapley, Churchstanton, Somerest, TA3 7QB UK as a substituent source.

3.4.1 Camellia phospholipids methodology

The camellia phospholipids as gums were isolated from extra virgin camellia oil by acid degumming process. In a typical procedure, 10.0 g of extra virgin tea oil was degummed with 500µl of 85% phosphoric acid. The mixtures were refluxed and stirred at 70 °C for 30 min. After reflux, extra virgin oil was centrifuged at 3500 rpm for 10 min in order to separate the crude gums and kept at room temperature. The crude gums were precipitated out at the bottom of the flask after 3-5 days. The phospholipids were purified from the crude gums by dissolving with chloroform. The phospholipids in chloroform soluble part were collected. The substances were evaporated and re-dissolved in chloroform as a stock solution at the concentration of 0.0043 g/mL.[34]

3.4.2 Determination of fatty acid compositions in extra virgin camellia oil

0.1 g of NaOH was dissolved with 4.56 g of methanol as Solution A. 10.0 g of extra virgin camellia oil was added into the Solution A. The mixtures were refluxed at 64 °C for 3 h. Then, the mixtures were centrifuged and washed with 60°C DI water for

2-3 times to remove the excess catalyst residues. The mixtures were placed under vacuum to remove the solvent at 110 ºC overnight.

3.4.3 Characterization of fatty acid compositions and camellia phospholipids

The camellia phospholipids in chloroform were characterized with various techniques to determine their functional groups and identify the type of phospholipids.

3.4.3.1 Gas chromatography (GC) technique.

The fatty acid composition was determined by calculations converting from triglyceride of extra virgin camellia oil to fatty acid methyl esters (FAMEs) using GC. The method determining the fatty acid compositions in extra virgin camellia oil was described in 3.4.1.

3.4.3.2 Fourier-transform infrared spectroscopy (FT-IR)

Fourier-transform infrared spectra of camellia oil before degumming process, camellia oil after degumming, and crude phospholipids were recorded with Nicolet 6700 FT-IR spectrometer equipped with a mercury-cadmium telluride (MCT) detector (Nicolet, USA) in order to determine the main functional groups of phospholipid molecules in comparison with a lecithin phospholipid standard.

3.4.3.3 Proton nuclear magnetic resonance (^{1}H-NMR) spectroscopy

The mixtures were characterized by Proton nuclear magnetic resonance (^{1}H-NMR) spectra on Bruker NMR spectrometer at 100 MHz to elucidate the structures of phospholipid molecules in comparison with lecithin. Camellia phospholipids were dissolved with chloroform-d ($CDCl_3$).

3.4.3.4 31-Phosphorus Nuclear magnetic resonance (^{31}P-NMR) spectroscopy

Phospholipids standard (L-α-phosphotidylcholine, lecithin) and camellia phospholipids were dissolved in 2:1 (v/v) chloroform-d ($CDCl_3$): methanol-d4 solvent containing triethyl phosphate as an internal standard.[44] The samples were characterized to determine the individual phosphorus by 31-Phosphorus Nuclear magnetic resonance spectroscope on Advance III HD Bruker at 202 MHz 27ºC.

3.5 Surface modification of as-synthsized TOPO-CdSe-ZnS QDs with camellia phospholipids

For the surface modification of QDs, as-synthesized TOPO-CdSe-ZnS quantum dots were modified with camellia phospholipids (PLs) by a micelle formation modified from a report by Hu. R in 2012.[41] 250 µL of phospholipids stock solution was dissolved with 2 mL of chloroform. The phospholipids solution was stirred for 30 min. The original TOPO-CdSe quantum dots were centrifuged at 3500 rpm for 10 min for removing of excess ligands. Then, the original QDs were precipitated with ethanol, and centrifuged at 4000 rpm for 10 min. The precipitated QDs were dispersed in chloroform (2.5×10^{-6} M). Then, the phospholipids solution was added drop-wise into the flask containing precipitated QDs, and the mixture was stirred under UV light for 30 min. The QDs/PL mixtures in chloroform were evaporated using a rotary evaporator under reduced pressure. The dried QDs/PL was slowly dissolved with 2 mL Tris-HCl buffer pH 10. Finally, the non-coating QDs and free PL were removed by centrifugation at 3500 rpm for 10 min. Then, the QDs/PL in Tris-HCl were dialyzed against the desired final buffers at 5500 rpm for 30 min by centrifuge filters for 30,000 molecular weight cut off (MWCO). The procedure for preparing phospholipids-coated TOPO-CdSe-ZnS QDs micelles was illustrated In Figure 3.1.

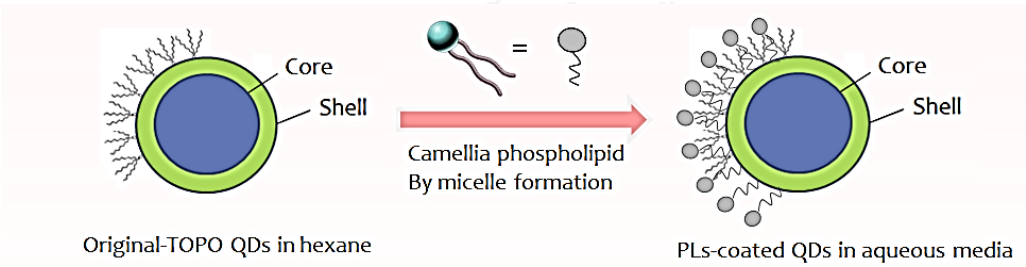

Figure 3.1: The process for preparing the aqueous soluble QDs using camellia phospholipids by micelle formation.

3.6 Characterization of the as-synthesized TOPO-CdSe-ZnS QDs and the phospholipids-coated TOPO-CdSe-ZnS QDs micelle

3.6.1 Ultraviolet-visible spectroscopy (UV-Vis spectroscopy)

The absorption spectra of the original TOPO-CdSe-ZnS QDs and the phospholipids-coated QDs were recorded on Varian Cary 50 UV-Vis spectrophotometer

(Varian, USA) from 400 nm to 700 nm at room temperature. The absorption at 470 nm was used to calculate the quantum yields of the particles.

3.6.2 Fluorescent spectroscopy

The emission spectra of the TOPO-CdSe-ZnS QDs and the phospholipids-coated QDs were recorded on a Varian Cary Eclipse spectrofluorometer (Varian, USA) from 510 nm to 800 nm at ambient temperature using an excitation wavelength at 480 nm. The data were used in calculation for quantum yields of the QDs.

3.6.3 Transmission electron microscope (TEM)

Size and shape of the TOPO-coated QDs and the phospholipids-coated TOPO-QDs were monitored using a transmission electron microscope with LEM-2010 microscope at accelerating voltage of 120 kV (Japan). For sample preparation, the samples were deposited by drop casting onto carbon film with 300 mesh copper grids.

3.6.4 Dynamic light Scattering (DLS)

Size distribution of the TOPO-coated QDs in hexane and the phospholipid-coated TOPO-QDs in milliQ were measured to obtain the Z-average and the polydispersity index (PdI) by a Zetasizer version 7.05, Malvern instrument.

3.6.5 Quantum yields (QYs)

We calculated the quantum yield of the original TOPO-QDs and the phospholipids-coated TOPO-QDs by comparing with Rhodamine 6G as the standard fluorescent dye. The calculation followed Equation 3.1[45].

$$Q = Q_R \left(\frac{m}{m_R}\right)\left(\frac{n^2}{n_R^2}\right)$$

Q = Quantum yield

m= Slope of the linear regression between area peak of fluorescent and absorbance

n = Refractive index of solvent

R = Quantum yield of Rhodamine 6G standard of 0.95[46]

3.7 Colloidal stability and cytotoxicity test

The original TOPO-QDs and the phospholipid**s**-coated TOPO-QDs were tested of colloidal stability and cytotoxicity. The two properties are important to determine before used to biological applications.

3.7.1 Colloidal stability

In this part, we studied two effects on the colloidal stability of phospholipids coated TOPO-CdSe-ZnS QDs (PL-coated QDs) including types of buffer solutions and the sizes of QDs. The phospholipid coated original TOPO-QDs in 1 M Tris pH 10 were dialyzed by centrifugal filter to change the aqueous media from 1 M Tris pH 10 to 0.01 M PBS pH 7.4. In the first experiment, we studied the stability of the phospholipid coated original TOPO-QDs in 1 M Tris pH 10 and 0.01 M PBS pH 7.4 with different sizes of QDs including green QDs, orange QDs and red QDs under the same concentration (A_{470}= 0.25). For the second experiment, we studied the stability of the PL-coated green QDs (the smallest particle) comparing with the PL-coated red QDs (the largest particle) with different types of aqueous media include 1 M Tris-HCl pH 10, MilliQ, 0.1 M PBS pH 10 and 0.01 M PBS pH 10. All the samples were kept in dark, and the data were collected periodically for about two months upon excitation at 470 nm, and emission wavelength of 510-800 by florescent spectroscopy as described in 3.6.2.

3.7.2 Cytotoxicity test

The cytotoxicity of the original TOPO-CdSe-ZnS QDs and the phospholipids coated CdSe-ZnS QDs of different sizes and the synthetic mPAAs-coated CdSe-ZnS QDs were investigated by measuring the cell viability using the methyl thiazol tetrazolium bromide (MTT) assay[47]. In this research, we used the three cell types including L929 mouse fibroblast cell line as connective tissue cell line[48], HaCaT keratinocyte as skin cell line[49] and Raw 264.7 cell as macrophage immune cell line. The cells were plated on 96 well-plates with concentration of 30,000 cells/well in 200µl DMEM (10%FBS, 1% streptavidin), and incubated for 24 h in a humidity hood at 37°C and 5%CO_2. On the next day, 100 µL of old DMEM media was eliminated and replaced with 100 µL of the new one. Then, the original TOPO-CdSe-ZnS QDs in milliQ, PLs-coated green QDs in milliQ, PLs-coated orange QDs in milliQ, PLs-coated red QDs in milliQ and mPAA-coated

green QDs in milliQ were added into respective well at final concentration of particles of 1 mg/mL, 0.1 mg/mL, and 0.01 mg/mL about 3 replicates) at the same pH 8. From the experiment, we observed the long-term cytotoxicity test (48 h and 72 h, plate cell of 5,000 cell/well) in a humidity hood at 37°c and 5%CO_2. After the cells were stimulated with particles, all plates was centrifuged at 300 rpm for 1min. 150 µL of the supernatants were eliminated and replaced with 150 µL of the flesh one. 20µL of MTT solution (12mM, 5mg/mL) was added into each well. The mixtures were incubated for 1-1.30 h depending on the cell types in a humidity hood. After incubated with MTT solution, the well plates was centrifuged at 300 rpm for 5min. A half of the supernatants were removed from the well, and 100 µL PBS was added for washing to remove the excess MTT solution for 2 times. Next, 150 µL of the media mixtures were removed, and 150 µL of DMSO was added for dissolving the formazan crystals. The percentage of cell viability was calculated from the absorbance of the media measured in a microplate reader at 570 nm.

3.7.3 Measurement of cytokine releasing

In this research, we collected the supernatants of the original TOPO-CdSe-ZnS QDs, the PLs-coated CdSe-ZnS QDs of different sizes and the synthesized polymer mPAA-coated CdSe-ZnS QDs from MTT assay in Raw 264.7 macrophage cell line. Then, we estimated the level of TNF-α, IL-6 and IL-1β cytokine production in their supernatants using enzyme-linked immunosorbent assay (ELISA) kits (Bio-legend, USA), according to the manufacturer's instructions.

CHAPTER IV
RESULTS AND DISCUSSION

In Chapter 4, we explained the results and discussion into two parts. In the first part, we focused on the fatty acid compositions of camellia oil and the extraction of phospholipid compounds. The phospholipid compounds were removed from the extra virgin camellia oil using 85% phosphoric acid by a degumming process. The camellia phospholipids were characterized by Fourier-transform infrared spectroscopy (FT-IR), Gas chromatography (GC), Proton nuclear magnetic resonance spectroscopy (^{1}H-NMR) and 31-Phosphorus Nuclear magnetic resonance spectroscopy (^{31}P-NMR).

4.1 The camellia phospholipids

Figure 4.1: Amount of camellia phospholipids (gums) when kept the extra virgin of camellia oil at room temperature.

The extra virgin of camellia oil was refluxed with 500 µl of 85% phosphoric acid at 70 °c for 30 min. After degumming, the extra virgin of camellia oil was separated into two parts including degumming camellia oil and pallets like gums. The gums were viscous black oil that precipitated at the bottom of flask after kept at room temperature for 3-5 days as shown in Figure 4.1. The percent yield of the camellia phospholipids was 1.69% w/w of total extra virgin of camellia oil.

The camellia gums were collected and dissolved in chloroform for eliminating chloroform insoluble because phospholipids or gums can dissolve in chloroform. Then,

the gums in chloroform was placed under vacuum, and was re-dissolved with chloroform for 2 times to remove the contaminants. Camellia phospholipids stock solutions were shown in Figure 4.2.

Figure 4.2: Preparation of camellia phospholipids (gums) stock solutions

4.2 The characterization of fatty acid compositions of camellia oil

4.2.1 Fatty acid compositions by Gas chromatography (GC) technique

Fatty acid	Percent yield (% yield)
C18:2n6c (Linoleic)	61.4539
C8:0 (Caprylic)	11.3248
C16:0 (Palmitic)	11.0395
C17:0 (Heptadecanoic)	5.6811
C20:5n3 (Eicosapentaenoic acid)	3.0272
C18:1n9c (Oleic)	2.8793
C22:0 (Behenic)	2.0529
*PUFA	1.9544
**SFA	0.7138

* (C18:2n6t + C18:3n6+ C18:3n3+ C20:4n6+ C22:1n9+C22:2)
** (C20:0+C23:0)

Table 4.1: Fatty acid compositions of extra virgin of camellia oil (*Camellia oleifera* Abel.). GC chromatogram of fatty acid methyl ester (FAME) of *Camellia oleifera* Abel oil (Camellia oil) were shown in Appendix A.

The fatty acid compositions of extra virgin of camellia oil were presented in Table 4.1. Fatty acid compositions of extra virgin of camellia oil were composed of 61.45% of linoleic acid, 11.32% of caprylic acid, 11.04% of palmitic acid, 5.6811% of

heptadecanoic acid, 3.0272% of eicosapentaenoic acid, 2.8793% of oleic acid and 2.0529% of beheic acid. The percentage of polyunsaturated fatty acid and saturated fatty acid were 1.9544% and 0.7138%, respectively In comparison with previous study, the refined camellia oil was reported to contain 82% of oleic acid, 7.9% of palmitic acid and 6.8% of linoleic acid.[50] Though different in composition due to the different sources, the total of unsaturated fatty acid was more than the total of saturated fatty acid. The results indicated that the extra virgin of camellia oil mostly consists of unsaturated fatty acid that are suitable for use as an edible cooking oil. In conclusion, the GC technique could be used for the characterization of fatty acid compositions of camellia oil that can imply the fatty acid compositions on hydrophobic tails of phospholipid compounds.

4.3 The characterization of camellia phospholipids

4.3.1 Fourier transforms infrared spectroscopy (FT-IR) technique

The FT-IR spectra of camellia oil before degumming (a), camellia oil after degumming (b), 90% L,-α-phosphatidylcholine (lecithin) from soybean as a standard phospholipid (c) and camellia phospholipids (d) were shown in Figure 4.3. The spectra of both the phospholipid standard and the camellia phospholipids were similar (Figure 4.3c and 4.3d). the camellia phospholipids exhibited characteristic signals of C-H stretching vibration at about 2849 cm^{-1} and 2919.13 cm^{-1}, the C=O group at about 1739.46 cm^{-1}, the C-H bending at about 1454.66 cm^{-1}, and the peaks of PO_2 and P-O-C at about 989.62 cm^{-1} and 1085.52 cm^{-1} similar to the lecithin phospholipid standard. Moreover, the spectra of both the camellia oil before degumming and the camellia oil after degumming were similar (Figure 4.3a and 4.3b). The strong peak at 2847.54 cm^{-1} and 2918.74 cm^{-1} were characterized as the C-H stretching vibration, the strong peak at 1739.46 cm^{-1} was indicative of the C=O group, the peak at 1459.11 cm^{-1} was attributed to the C-H bending, and the peak at 1156.50 cm^{-1} was assigned to stretching vibration of the C-O ester group.[51] Normally, the FT-IR spectra of phospholipids were observed in the regions of PO_2 and P-O-C vibration at about 970-1200 cm^{-1}.[52] Therefore, the FT-IR peaks of camellia phospholipid compounds in camellia oil before degumming process were absent because the camellia oil before degumming process

is mostly phospholipids are mostly composed of triglycerides.[53] The results indicated that 85% of phosphoric acid could extract the residual phosphorus or phospholipids from the camellia oil as previously reported.[34] In addition, the crude camellia phospholipids comprised C-H bonding, carbonyl group(C=O), PO_2, and P-O-C bond as expected for phospholipid compounds.

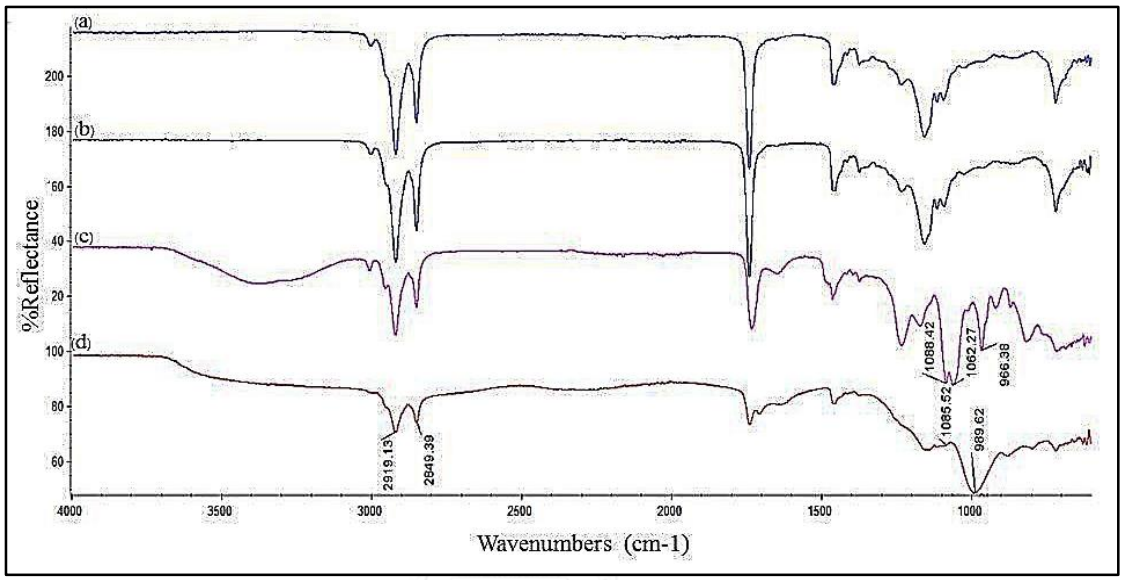

Figure 4.3: FT-IR spectra of (a) camellia oil before degumming, (b) camellia oil after degumming, (c) 90% L,α-phosphatidylcholine (lecithin) from soybean as a phospholipid standard, and (d) camellia phospholipids (PLs).

4.3.2 Proton nuclear magnetic resonance spectroscopy (^{1}H-NMR)

The camellia phospholipids that were extracted from the extra virgin oil were characterized to determine the structure by a proton nuclear magnetic resonance spectroscopy (^{1}H-NMR).

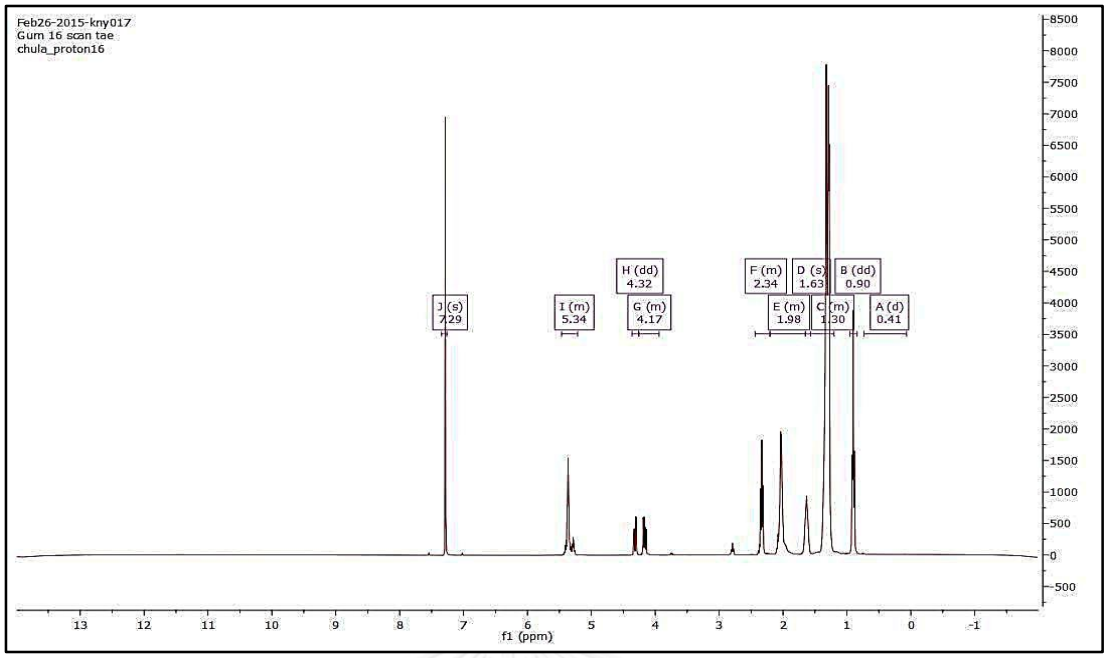

Figure 4.4: ^{1}H-NMR spectra of camellia phospholipids from 85% phosphoric acid degumming process of extra virgin of camellia oil in $CDCl_3$.

^{1}H-NMR technique is a technique for determine the structure of camellia phospholipid molecules. The phospholipid molecule can be simplified by the three groups of proton signals including the photons of the fatty acid chain, the protons of the glyceride residue and methylene groups of the polar heads, and protons bounded to heteroatoms.[54] The ^{1}H-NMR spectra of camellia phospholipids are shown in Figure 4.4. The spectra of fatty acid chain of phospholipids can be interpreted by direct comparison with the ^{1}H-NMR spectra of triglyceride. The all unsaturated acyl chains (CH=CH, and CH_2-CH=CH) were appeared at 5.34 ppm and 1.98 ppm. The all acyl chains ($(CH_2)_n$) were observed at 1.30 ppm. The all acyl chains of (CH_2COOH), which were interpreted to free fatty acid, were observed at 1.63 and 2.34 ppm. The doublet of doublet peak at 0.90 ppm was interpreted to the all acyl chain except linolenyl. In contrast, the signal peak at 2.79 ppm was assigned as the linolenyl and linoleyl chains. These proton signals as in the phospholipids. The glycerol residues (CH_2-OCOR) was recorded at 4.18 ppm and 4.32 ppm[55]. Normally, the signal of glyceride residue was observed as a multiplet at 4.86 ppm due to 4 neighboring methylene protons. This experiment, the glyceride residue signal was not observed obliviously because the absorption of methylene proton is ambiguous by more signals of protons in some

unsaturated fatty acid phospholipid compound. In contrast, the signal of glycerol (CH2-OCOR) was detected at 4.32 ppm as glycerol of phosphatidylcholine. The ^{1}H-NMR signal was interpreted as proton of the glyceride residues. In conclusion, the results from 1H-NMR indicated that acid degumming process could remove the phospholipid residues from extra virgin camellia oil.

4.3.3 31-Phosphorus nuclear magnetic resonance spectroscopy (^{31}P-NMR)

The ^{31}P-NMR technique is fast and accuracy technique to qualitatively analyze a mixture phospholipids in biological sources.[8] We used this technique for analyze the phosphorus compounds for determining the chemical structure of the camellia phospholipids that were extracted from extra virgin of camellia oil.

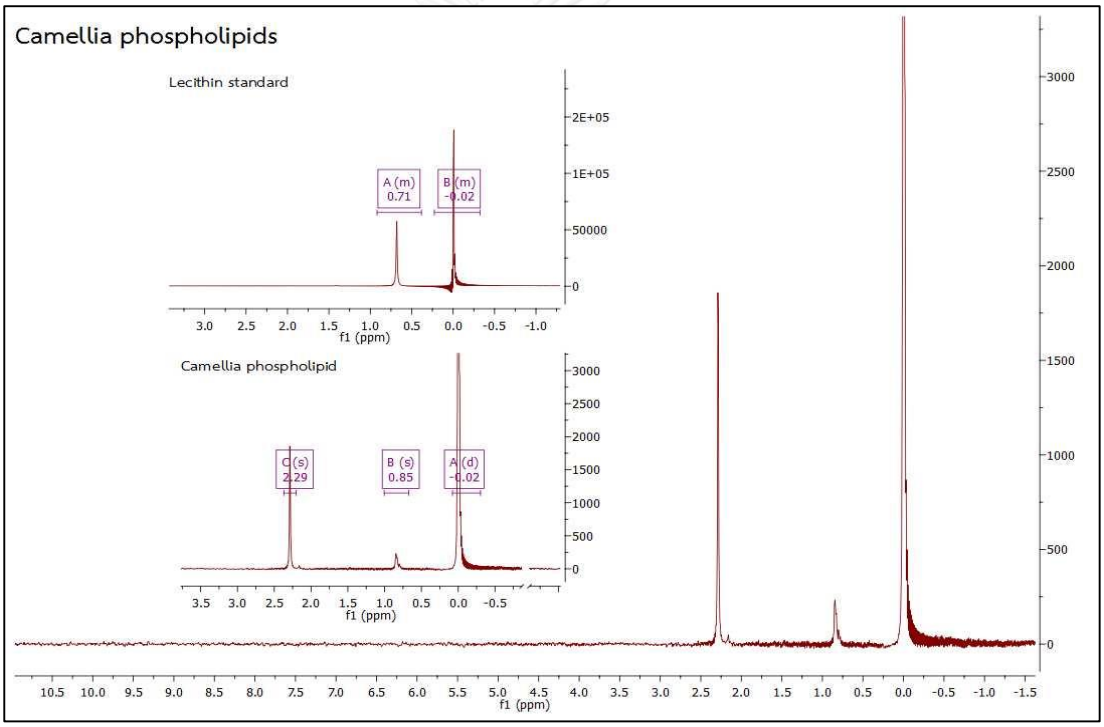

Figure 4.5: ^{31}P-NMR spectra of crude camellia phospholipids from degumming process of extra virgin camellia oil with 85% phosphoric acid which dissolved in $CDCl_3$:CD_3OD: 2:1 containing triethyl phosphate at 27°c, 202 MHz.

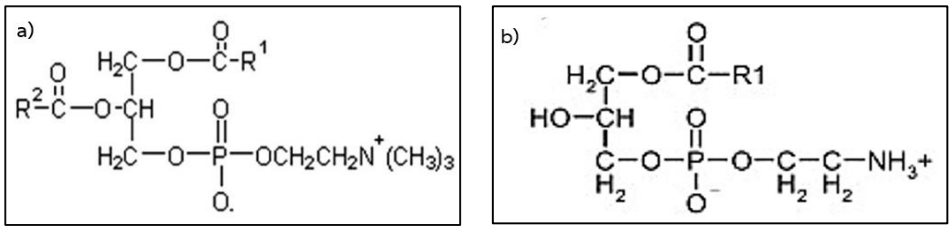

Figure 4.6: Chemical structures of (a) phosphatidylcholine (PC) and (b) lysophosphatidylethanolamine (LPE). R1 and R2 represent fatty acid chain.[56, 57]

The camellia phospholipids were dissolved in $CDCl_3$:CD_3OD at ratio 2:1 containing the internal reference (triethyl phosphate), and were analyzed by ^{31}P-NMR technique at 27°C. The ^{31}P-NMR spectra of crude camellia phospholipids were shown in Figure 4.5. The chemical shift value of camellia phospholipids from extra virgin of camellia oil showed two species of phospholipids, as the signal were observed at 0.85 ppm and 2.29 ppm. The signal at 0.85 ppm was characterized a phosphatidylcholine when compared with lecithin standard (L-α-phosphatidylcholine), and the signal at 2.29 ppm was assigned as a lysophosphatidylethanolamine when compared with previous study.[44] The chemical structure of phosphatidylcholine (PC) and lysophosphatidylethanolamine (LPE) were shown in Figure 4.6. The chemical shifts of pattern in 31P-NMR depend on the concentration of the sample, type of solvent and the presence of other compounds. In the same compound , the chemical shift could vary at least 1 ppm, especially for phosphate groups (P=O) because the external standard does not take into account of the bulk properties of the samples.[58] The results indicated that the camellia phospholipids were composed of the phosphatidylcholine and lysophosphatidylethanolamine.

4.4 Synthesis and characterization of the original TOPO-CdSe-ZnS QDs

In this section, we focused on the synthesis and characterization of the original TOPO-CdSe-ZnS QDs and the camellia phospholipids-coated CdSe-ZnS QDs (the PLs-coated CdSe-ZnS QDs).

4.4.1 Synthesis of the original TOPO-CdSe-ZnS QDs in different sizes

Figure 4.7: The different sizes of the original TOPO-CdSe-ZnS QDs including green CdSe-ZnS QDs, orange CdSe-ZnS QDs and red CdSe-ZnS QDs in hexane under UV irradiation.

We synthesized the different sizes including green QDs, orange QDs and red QDs of the original CdSe-ZnS QDs by hot injection with stabilization with triocylphosphine oxide (TOPO) as a capping ligand. The Cd and Se precursors were rapidly injected into hot surfactants/solvents mixture at 360 °c. For green CdSe QDs, the reaction was suddenly stopped after the injection. For orange and red CdSe QDs, the reaction was held at the injection temperature for at least 1 min for orange QDs and 3-5 min for red CdSe QDs. Next step, we over-coated ZnS shell onto the surface of CdSe QDs. CdSe cores in hexane were injected into Zn precursor at 60 °C. Then, the hexane was evaporated, and triocylphosphine sulfide (TOPS) solution was slowly dropped at 150 °C. All three sizes of the resulted CdSe-ZnS QDs were also passivated with TOPO on their surfaces and exhibited high fluorescent under UV irradiation[43] as shown in Figure 4.7.

4.5 Optical properties of the original TOPO-CdSe-ZnS QDs and the PLs-coated CdSe-ZnS QDs in different sizes

4.5.1 Absorption spectra of the original TOPO-CdSe-ZnS QDs and the PLs-coated CdSe-ZnS QDs in different sizes

The different sizes of the original TOPO-CdSe-ZnS QDs including green QDs, orange QDs, and red QDs in hexane and the phospholipids-coated CdSe-ZnS QDs of different sizes (PLs-coated CdSe-ZnS QDs) in 1M Tris pH10 were characterized by UV-Vis spectroscopy as shown in Figure 4.8. The original green TOPO-CdSe-ZnS QDs were

obliviously observed three characteristic UV absorption peaks at 450 nm, 515 nm, and 546 nm. The original orange TOPO-CdSe-ZnS QDs have three characteristic UV absorption peaks at 475 nm, 555 nm, and 570 nm, and the original red TOPO-CdSe-ZnS QDs have two characteristic UV absorption peaks at 500 nm, and board peak at 600 nm. Then, the original TOPO-CdSe-ZnS QDs were modified with camellia phospholipids in chloroform by micelle-like formation. After chloroform was evaporated by a rotary evaporation, the thin films of PLs-coated CdSe-ZnS QDs were formed, and then the 1M Tris pH10 as aqueous media was dropped to dissolve the thin film. We obtained slightly turbid PLs-coated CdSe-ZnS QDs. Normalized absorption spectra of the camellia phospholipids coated the original TOPO-CdSe-ZnS QDs in 1 M Tris pH 10 were shown in Figure 4.9. The absorption spectra of the PLs-coated green CdSe-ZnS QDs have two characteristic UV absorption peaks at 455 nm, 500 nm. The absorption spectra of the PLs-coated orange CdSe-ZnS QDs observed three characteristic UV absorption peaks at 475 nm, 537 nm, 570 nm, and the absorption spectra of the PLs-coated red CdSe-ZnS QDs observed two characteristic UV absorption peaks at 545nm and 620 nm. Both of the three original TOPO-CdSe-ZnS QDs and the PLs-coated CdSe-ZnS QDs in three sizes showed the board excitation spectra, which are a unique characteristic of quantum dots. After modification with camellia phospholipids, the UV absorption peaks were slightly decreased in absorbance, but retained the UV absorption characteristic when compared with the original TOPO-CdSe-ZnS QDs in hexane. The decreases in the characteristic absorption peaks of the PLs-coated CdSe-ZnS QDs were partly due to some QDs aggregation, some attachment of phospholipid molecules that were packing themselves into small particles to bound the QD surfaces, surface degradation of QDs upon transferring from the organic phase into aqueous phase, and elimination of PLs-QDs through membrane filters during the dialysis process The results indicated that the TOPO-CdSe-ZnS QD surfaces experienced some changes, and it was likely that the TOPO-CdSe-ZnS QDs were modified with camellia phospholipids and became PLs-QDs micelles.

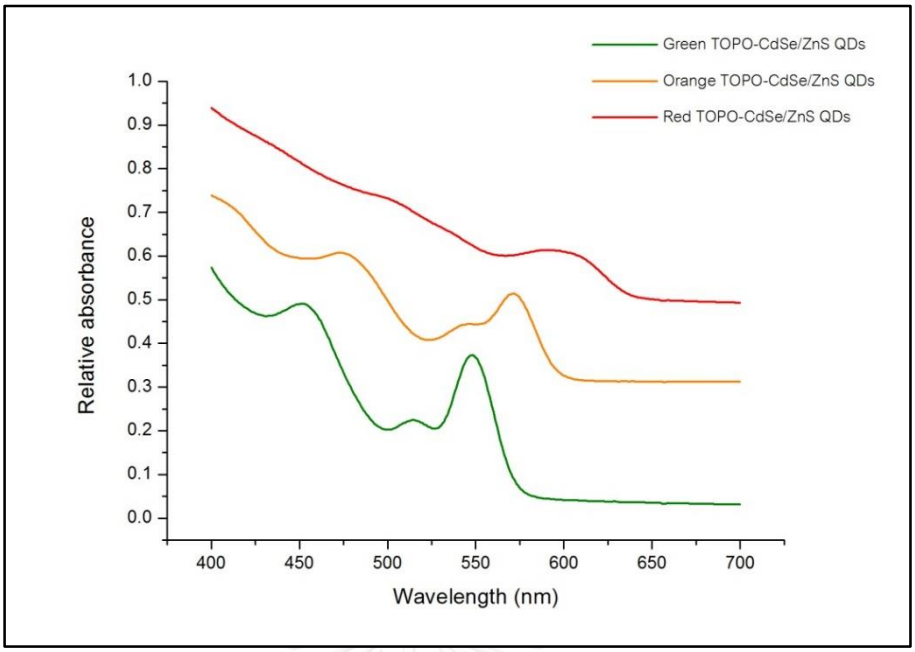

Figure 4.8: Normalized absorption spectra of the original TOPO-CdSe-ZnS QDs in hexane; green QDs (green line), orange QDs (orange line), and red QDs (red line).

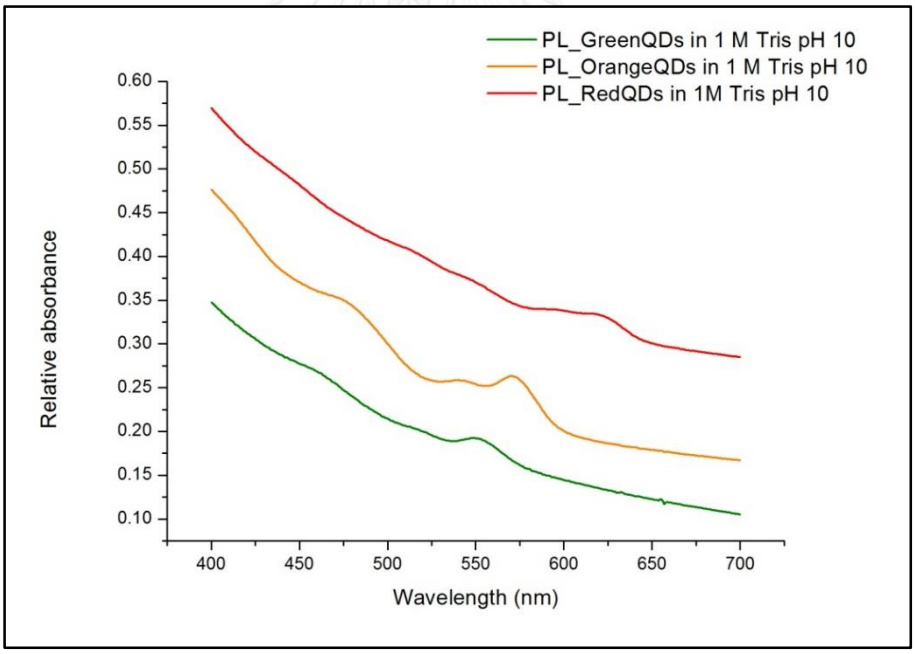

Figure 4.9: Normalized absorption spectra of the camellia phospholipids coated the original CdSe-ZnS QDs (PLs-coated CdSe-ZnS QDs) in 1 M Tris pH 10; PLs-coated green QDs (green line), PLs coated orange QDs (orange line), and PLs-coated red QDs (red line).

4.5.2 Fluorescent spectra of the original TOPO-CdSe-ZnS QDs and the PLs-coated CdSe-ZnS QDs in different sizes

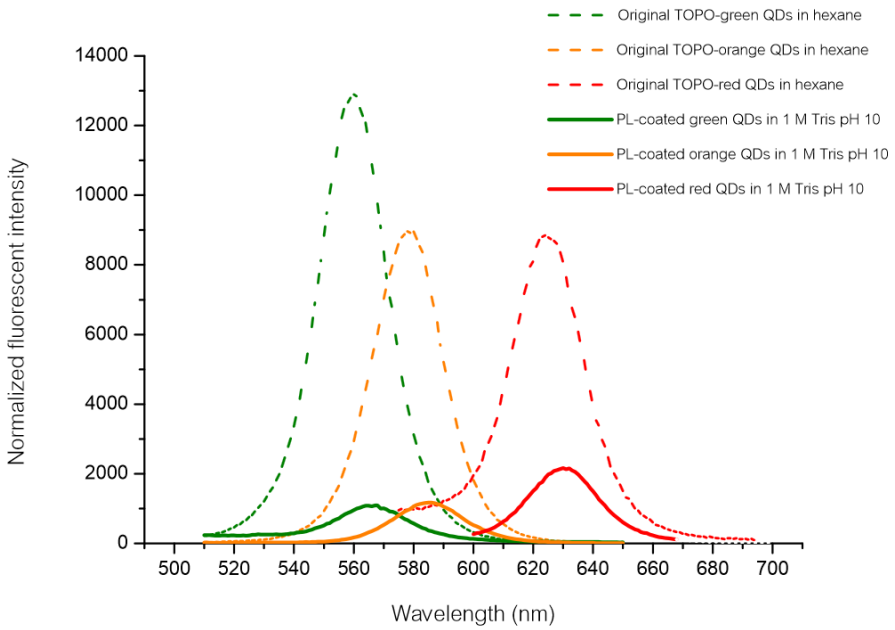

Figure 4.10: Normalized fluorescent intensity of the original TOPO-CdSe-ZnS QDs in hexane (Dash line) and the phospholipids coated the original CdSe-ZnS QDs (Solid line) in different sizes (green QDs, orange QDs and red QDs).

The original TOPO-CdSe-ZnS QDs after modified with phospholipids were dissolved in 1 M Tris buffer pH 10. The PLs-coated CdSe-ZnS QDs solution was slightly turbid and retained the fluorescent intensity when compared with the original TOPO-CdSe-ZnS QDs under UV light. The emission spectra were measured under the excitation wavelength at 470 nm and the emission wavelength at 510-800 nm. In Figure 4.10 and Table 4.2, the original green TOPO-CdSe-ZnS QDs, the original orange TOPO-CdSe-ZnS QDs, and the original red TOPO-CdSe-ZnS in hexane showed the highest quantum yield about 33.44 %, 24.29 %, and 33.36 % with the emission peaks at 560 nm, 578 nm, and 628 nm, respectively. After the original TOPO-CdSe-ZnS QDs in different sizes were modified with camellia phospholipids, the PLs-coated green CdSe-ZnS QDs in 1 M Tris pH 10, the PLs-coated orange CdSe-ZnS QDs in 1M Tris pH 10, and the PLs-coated red CdSe-ZnS QDs in 1 M Tris pH 10 exhibited moderately fluorescent intensity when compared with the original TOPO CdSe-ZnS QDs in hexane. The

quantum yield of the PLs-coated green CdSe-ZnS QDs in 1 M Tris pH10, the PLs-coated orange CdSe-ZnS QDs in 1 M Tris pH10, and the PLs-coated red CdSe-ZnS QDs in 1 M Tris pH 10 were 2.84%, 1.30%, and 2.43% with the emission peaks at 566 nm, 585 nm, and 631 nm. After modification, the emission wavelength of the PLs-coated CdSe-ZnS QDs of three sizes were similar to the emission wavelength of the original TOPO-CdSe-ZnS QDs of the same sizes. The results indicated that the size of CdSe/Zn QDs did not change obliviously upon modification with camellia phospholipids by micelle formation. In contrast, the original TOPO-CdSe-ZnS QD in hexane exhibited highest quantum yields, while the quantum yields of the PLs-coated CdSe-ZnS QDs in 1 M Tris pH 10 was decreased for all three sizes of QDs. The reason for this observation were likely because the surfaces of QDs were covered with amphiphilic phospholipids that could cause the trap sites and surface passivation during modification process[59], and the phospholipids may degrade during the modification of QDs on their surface.[60] The results indicated that the original TOPO-CdSe-ZnS QDs were modified their surface with camellia phospholipids. The PLs-coated CdSe-ZnS QDs were not completely quenched in fluorescence signals and could also be use the camellia phospholipids to prepare the quantum dots in media.

4.6 Quantum yields, size distribution and TEM images

Particles	Original green QDs	Original orange QDs	Original red QDs	PLs-coated green QDs	PLs-coated orange QDs	PLs-coated red QDs
Quantum yield (%)	33.44	24.29	33.36	2.84	1.30	2.43

Table 4.2: Quantum yield values of the original TOPO-CdSe-ZnS QDs in hexane and the PLs-coated CdSe-ZnS QDs in MilliQ of different sizes as calculated by equation 1.

Particles	Original green QDs	Original orange QDs	Original red QDs	PLs-coated green QDs	PLs-coated orange QDs	PLs-coated red QDs
Size distribution (PdI)	0.212	0.565	0.547	0.213	0.214	0.231
Z-Average (d.nm)	10.48	1449	1749	119.4	151.5	143.9
Particle diameters (nm)	2.67	3.34	4.48	2.72	3.02	4.13

Table 4.3: Size distribution, Z-average, particle diameters of the original TOPO-CdSe-ZnS QDs in hexane and the PLs-coated CdSe-ZnS QDs in MilliQ of different sizes as measured by the Zetasizer version 7.05, Malvern instrument and transmission electron microscope (TEM).

Particle sizes of the original TOPO-CdSe-ZnS QDs and the PLs-coated QDs in different sizes were characterized by transmission electron microscopy (TEM). In Figure 4.11 and Table 4.3, the original green TOPO-CdSe-ZnS QDs, the original orange TOPO-CdSe-ZnS QDs and the original red TOPO-CdSe-ZnS QDs in hexane were observed as the monodisperse dot shapes (PdI ≤ 0.7), and the particle sizes was 2.67 nm, 3.34 nm, and 4.48 nm in diameters, respectively. After the original TOPO-CdSe-ZnS QDs in different sizes were modified with camellia phospholipids, the PLs-coated green CdSe-ZnS QDs, the PLs-coated orange CdSe-ZnS QDs, and the PLs-coated red CdSe-ZnS QDs in milliQ retained monodispersity without non-aggregation(PdI ≤ 0.7).[61] The particle sizes of PLs-coated green CdSe-ZnS QDs, the PLs-coated orange CdSe-ZnS QDs, and the PLs-coated red CdSe-ZnS QDs in milliQ were 2.72 nm, 3.02 nm, and 4.13 nm, respectively. The particle sizes of the original TOPO-

CdSe-ZnS QDs are larger than the PLs-coated CdSe-ZnS QDs likely because some ZnS shell were etched during the process. The results indicated that the original TOPO-CdSe-ZnS QDs were modified with camellia phospholipids, and the PLs-coated CdSe-ZnS QDs are slightly decreased in sizes, mono dispersed in sizes but unchanged in shapes.

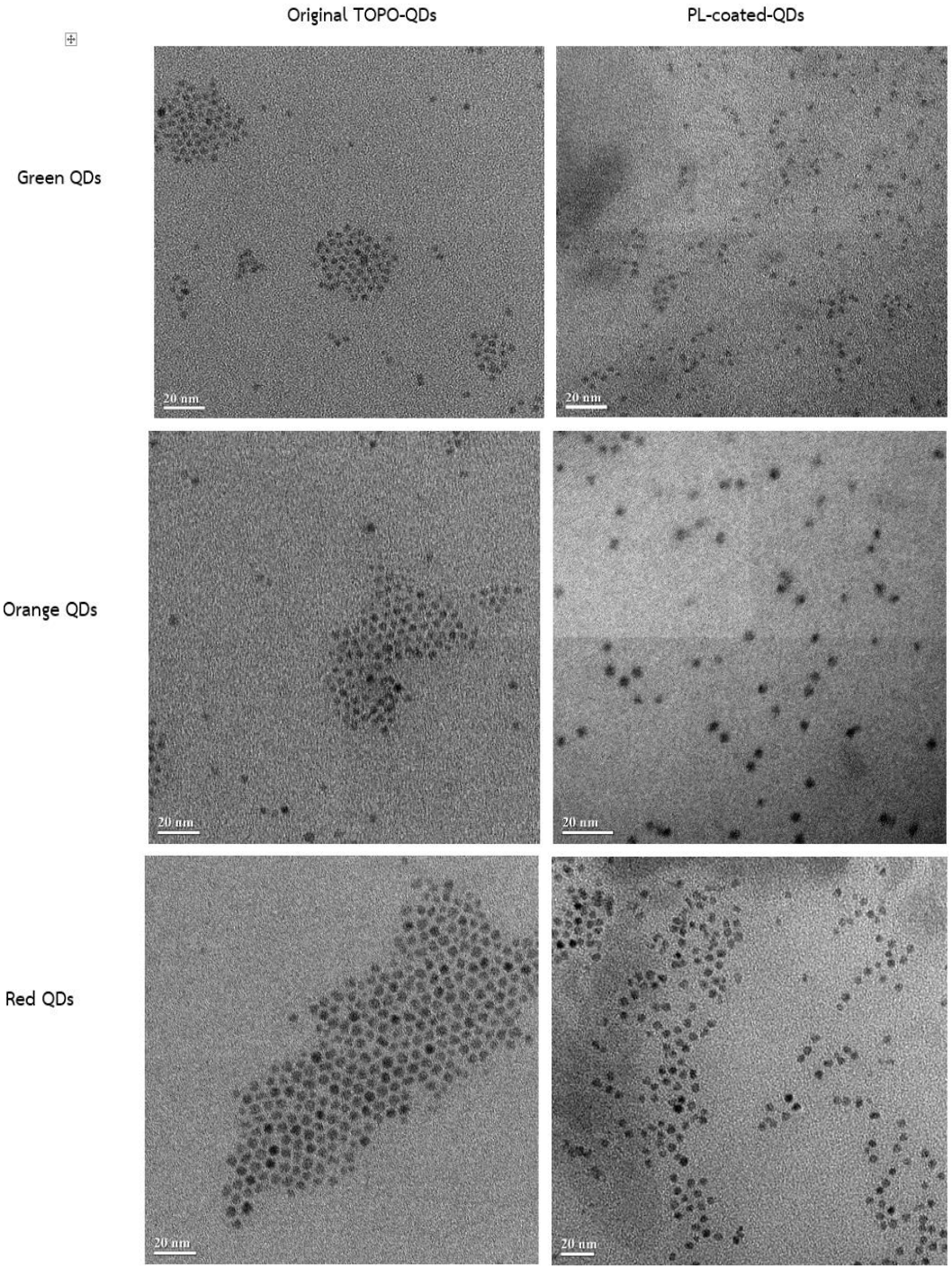

Figure 4.11: TEM images of the original TOPO-CdSe-ZnS QDs in hexane (left), and the phospholipid coated CdSe-ZnS QDs dispersed in milliQ after kept for a day (right).

4.7 Stability test

The colloidal stability of phospholipids-coated CdSe-ZnS QDs were determined by fluorescent spectroscopy which calculated the peak area of fluorescent spectrum at time intervals for 2 months. The samples were kept in room temperature against the light. For the experiments, we estimated two effects on colloidal stability, which are effect of different sizes of QDs in the same aqueous media and effect on various aqueous media for the same sizes of QDs.

4.7.1 Effect of QDs sizes on stability

The original TOPO-CdSe-ZnS QDs were modified with camellia phospholipids that were dissolved in 1M Tris pH10. Then, the PLs-coated CdSe-ZnS QDs in 1M Tris pH10 were dialyzed by centrifugal filters for changing the Tris buffer to 0.01 M PBS pH 7.4. When the aqueous media was changed, the PLs-coated CdSe-ZnS QDs in 0.01 M PBS at pH 7.4 were slightly turbid and decreased in the fluorescent intensity. We compared the PLs-coated CdSe-ZnS QDs in 1 M Tris pH 10 and the PLs-coated CdSe-ZnS QDs in 0.01 M PBS pH 7.4 of different sizes of QDs include green QDs, orange QDs and red QDs.

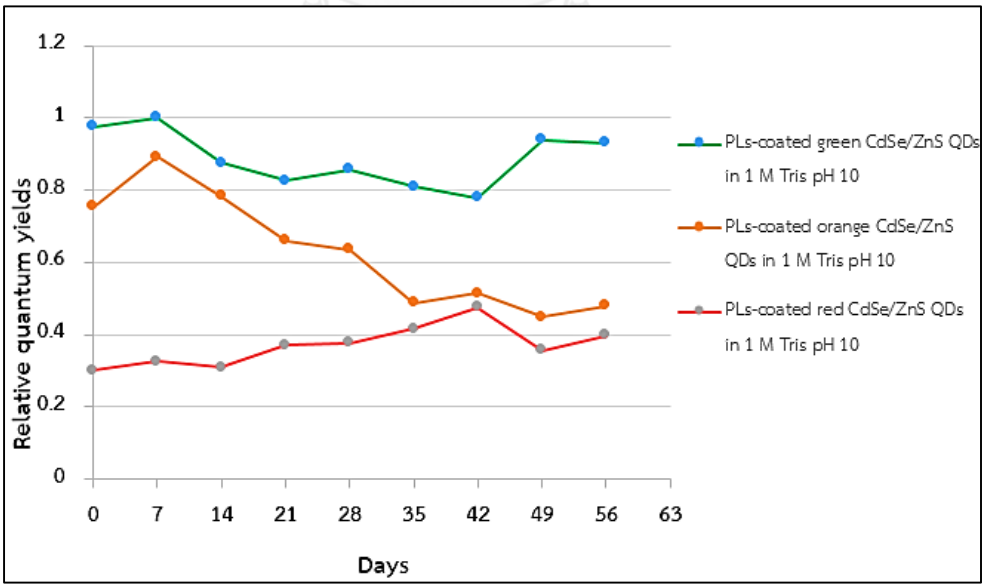

Figure 4.12: The colloidal stability of the PLs-coated CdSe-ZnS QDs in 1 M Tris pH 10 of the different sizes of QDs including the PLs-coated green CdSe-ZnS QDs (green line),

the PLs-coated orange CdSe-ZnS QDs (orange line) and the PLs-coated red CdSe-ZnS QDs (red line).

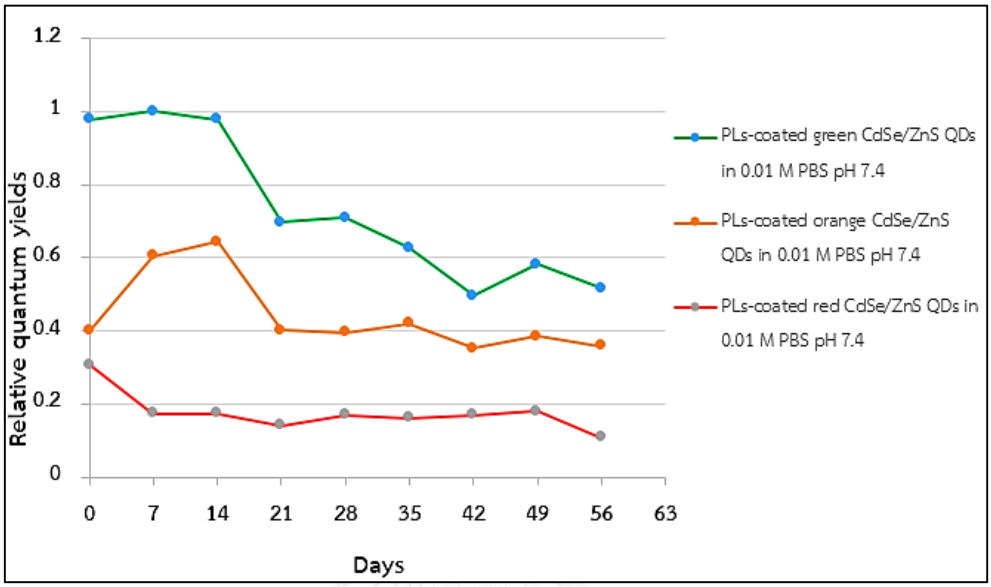

Figure 4.13: The colloidal stability of the PLs-coated CdSe-ZnS QDs in 0.01M PBS pH 7.4 of the different sizes of QDs including the PLs-coated green CdSe-ZnS QDs (green line), the PLs-coated orange CdSe-ZnS QDs (orange line) and the PLs-coated red CdSe-ZnS QDs (red line).

In Figure 4.12, the PLs-coated green and red CdSe-ZnS QDs in 1 M Tris pH 10 were slightly decreased in relative quantum yield. While, the PLs-coated orange CdSe-ZnS QDs in 1 M Tris pH 10 were dramatically decreased in the relative quantum yield after 7 days. Furthermore, in Figure 4.13, the relative quantum yield of PLs-coated green CdSe-ZnS QDs in 0.01 M PBS pH 7.4 still retained for 14 days before dramatically decreased on Days 15. In the same way, the relative quantum yield of the PLs-coated orange CdSe-ZnS QDs in 0.01 M PBS pH 7.4 were constantly for 2 weeks before the relative quantum yield were slightly dropped at Days 15. Whereas, the PLs-coated red CdSe-ZnS QDs in 0.01 M PBS pH 7.4 were rapidly declined in the fluorescent intensity after kept for 3 days, and changed the emission wavelength due to aggregation of QDs. The results indicated that the PLs-coated green CdSe-ZnS QDs were more stable than

the PLs-coated orange CdSe-ZnS QDs and the PLs-coated red CdSe-ZnS QDs in basic media and neutral media for 2 weeks.

4.7.2 Effect of types of aqueous media

In this experiment, we determined the colloidal stability of the PLs-coated CdSe-ZnS QDs in smallest sizes (green QDs) and the PLs-coated CdSe-ZnS QDs in largest sizes (red QDs) in different aqueous media. After aqueous media were changed, the PLs-coated green CdSe-ZnS QDs in milliQ, the PLs-coated green CdSe-ZnS QDs in 0.01 M PBS pH10 and the PLs-coated green CdSe-ZnS QDs in 0.1 M PBS pH10 were continuously decreased the fluorescent intensity when compared with the PLs-coated green QDs in 1 M Tris pH 10. In the same ways, the PLs-coated red CdSe-ZnS QDs in milliQ, the PLs-coated red CdSe-ZnS QDs in 0.01 M PBS pH 10 and the PLs-coated red CdSe-ZnS QDs in 0.1 M PBS pH 10 were slightly decreased in the fluorescent intensity when compared the PLs-coated red CdSe-ZnS QDs in 1 M Tris pH10.

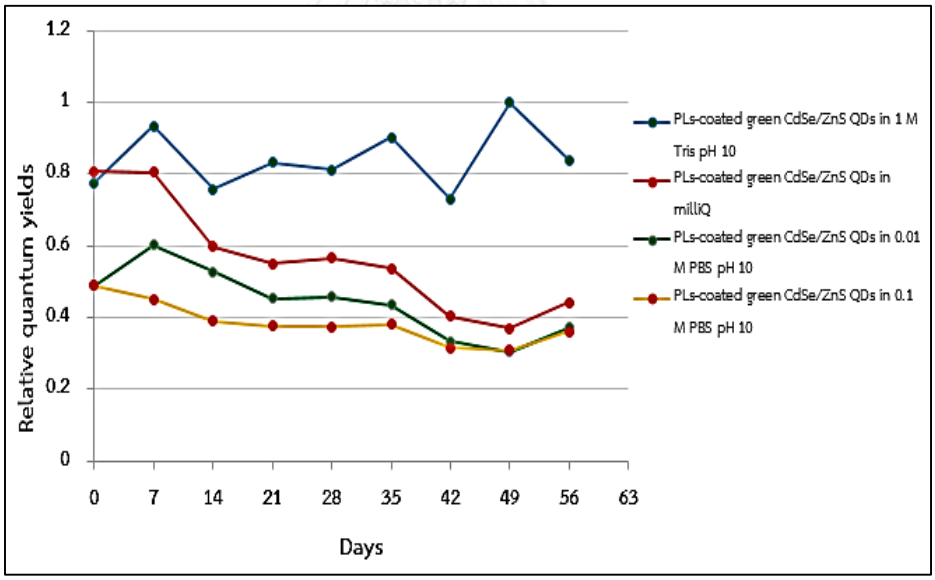

Figure 4.14: The colloidal stability of the PLs-coated green CdSe-ZnS QDs (the smallest sizes studied) in various aqueous media including in 1 M Tris pH 10 (blue line), MilliQ (red line), 0.1 M PBS pH 10 (grey line) and 0.01 M PBS pH 10 (yellow line).

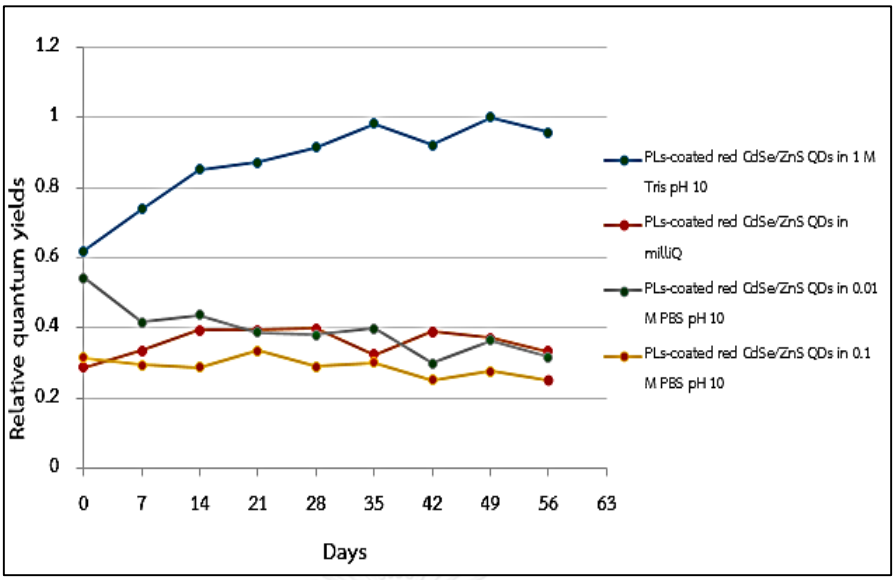

Figure 4.15: The colloidal stability of the PLs-coated red CdSe-ZnS QDs (the largest sizes studied) in various aqueous media including 1 M Tris pH 10 (blue line), MilliQ (red line), 0.1 M PBS pH 10 (grey line) and 0.01 M PBS pH 10 (yellow line).

In Figure 4.14, the colloidal stability of the PLs-coated green CdSe-ZnS QDs in milliQ, of the PLs-coated green CdSe-ZnS QDs in 0.01 M PBS pH 10 and the PLs-coated green CdSe-ZnS QDs in 0.1 M PBS pH 10 were slightly decreased in the relative quantum yields when compared the PLs-coated green CdSe-ZnS QDs in 1M Tris pH 10. In contrast, in Figure 4.15, the PLs-coated red CdSe-ZnS QDs in milliQ, the PLs-coated red CdSe-ZnS QDs in 0.01 M PBS pH 10 and the PLs-coated red CdSe-ZnS QDs in 0.1 M PBS pH 10 were constant in the relative fluorescent intensity for 2 months, but the emission wavelength was changed. The results indicated that the PLs-coated with smallest CdSe-ZnS QDs was stable in basic aqueous media such as 1M Tris pH 10 for more 2 months because the PLs coated with smallest QDs are unchanged in the emission wavelength, maintained strongly fluorescent intensity and non-aggregation. However, for biological applications, the QDs should be dispersible in aqueous media at neutral pH. For both experiments, the PLs-coated green CdSe-ZnS QDs in 0.01 M PBS pH 7.4 were stable about 2 weeks, and suitably used for applications within limited time after preparation.

4.8 Cytotoxicity

The cytotoxicity of the original TOPO-CdSe-ZnS QDs and the PLs-coated CdSe-ZnS QDs were determined by studying the percent of cell viability using the methyl thiazol tetrazolium bromide (MTT) assay. We investigated cytotoxicity of PLs-CdSe-ZnS QDs for two objectives. First, we compared the cytotoxicity of PLs-coated CdSe-ZnS QDs of different sizes in milliQ with the original TOPO-CdSe-ZnS QDs in milliQ. Then, we compared the cytotoxicity of the synthesized polymer mPAA-coated CdSe-ZnS QDs with the PLs-coated CdSe-ZnS QDs as natural polymers in green QDs. The experiments, we used three types of cell line including HaCaT human keratinocyte, mouse fibroblast (L929), and 264.7 raw cell at 24h, 48h, and 72h incubation times.

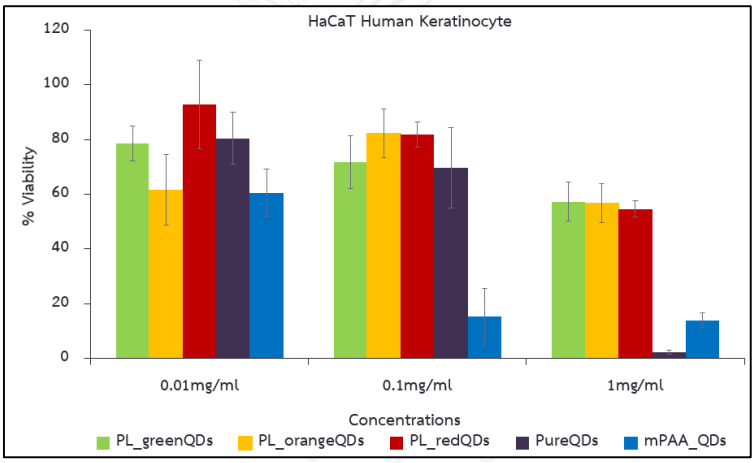

Figure 4.16: The percentages of cell viability of the PLs-coated CdSe-ZnS QDs in milliQ in different sizes compared with the original TOPO-CdSe-ZnS QDs in milliQ and the mPAA-coated green CdSe-ZnS QDs in milliQ incubated with HaCaT human keratinocytes for 24 h.

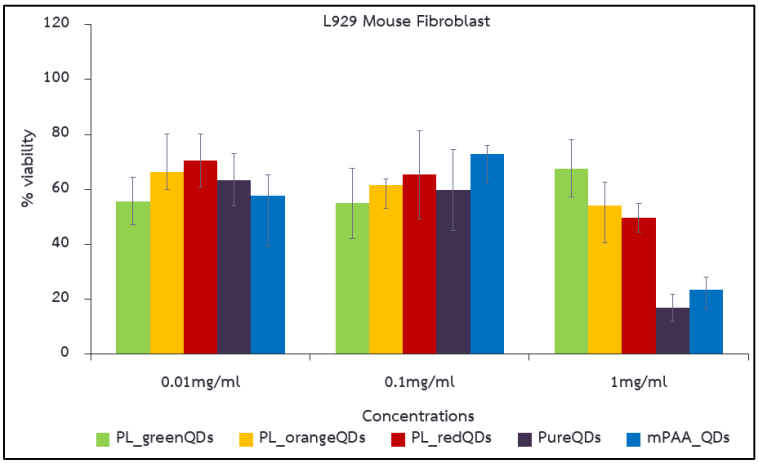

Figure 4.17: The percentages of cell viability of the PLs-coated CdSe-ZnS QDs in milliQ in different sizes compared with the original TOPO-CdSe-ZnS QDs in milliQ and the mPAA-coated green CdSe-ZnS QDs in milliQ incubated with L929 mouse fibroblast for 24 h.

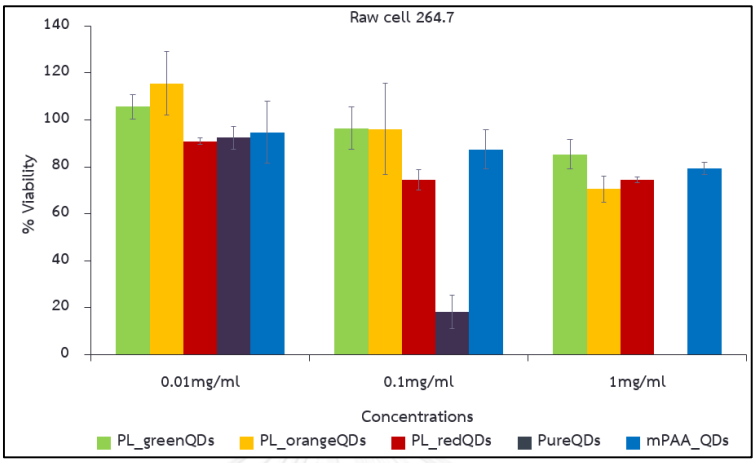

Figure 4.18: The percentages of cell viability of the PLs-coated CdSe-ZnS QDs in milliQ in different sizes compared with the original TOPO-CdSe-ZnS QDs in milliQ and the mPAA-coated green CdSe-ZnS QDs in milliQ incubated with raw cell for 24 h.

The cytotoxicity of the PLs-coated with three sizes of CdSe-ZnS QDs in milliQ, the original TOPO-CdSe-ZnS QDs in milliQ and the mPAA-coated CdSe-ZnS QDs in milliQ were evaluated the cell viability. As shown in Figure 4.16, when HaCaT human keratinocyte was exposed to the CdSe-ZnS QDs for 24h, the PLs-coated with three sizes of CdSe-ZnS QDs and the original TOPO-CdSe-ZnS QDs gave 80% of cell viability at low concentrations of 0.1mg/mL and 0.01mg/mL. On the other hand, the PLs-coated with three sizes of CdSe-ZnS QDs yielded 60% of cell viability, but cell viability after exposed to the original TOPO-CdSe-ZnS QDs was dramatically decreased at high concentration of 1mg/mL. Then, the cell viability of the mPAA-coated green CdSe-ZnS QDs were decreased significantly when compared with that of the PLs-coated green CdSe-ZnS QDs at high concentration of 1mg/mL and 0.1mg/mL for 24h incubation.

In Figure 4.17, when L929 mouse fibroblast was exposed to the CdSe-ZnS QDs for 24h, the cell viability of both the PLs-coated with three sizes of CdSe-ZnS QDs and the original TOPO-CdSe-ZnS QDs were slightly increased to 70% at low concentrations of 0.1mg/mL and 0.01mg/mL. In contrast, the cell viability of the original TOPO-CdSe-

ZnS QDs were decreased significantly, but the cell viability of the PLs-coated with three sizes of CdSe-ZnS QDs were increased to 70% at high concentration of 1mg/mL. Then, the cell viability of the mPAA-coated green CdSe-ZnS QDs were decreased significantly when compared with that of the PLs-coated green CdSe-ZnS QDs a high concentration of 1mg/mL for 24h incubation.

In Figure 4.18, when 264.7 raw cell were exposed with the CdSe-ZnS QDs for 24h, the cell viability of PLs-coated with three sizes of CdSe-ZnS QDs were increased to 80% at all concentrations, but the cell viability of original TOPO-CdSe-ZnS QDs were increased to 80% at low concentration of 0.01mg/mL. On the other hand, the cell viability of the original TOPO-CdSe-ZnS QDs were dramatically decreased at high concentration of 0.1mg/mL and 1mg/mL. However, the cell viability of the mPAA-coated green CdSe-ZnS QDs were not different significantly when compared with the PLs-coated green CdSe-ZnS QDs at all concentration for 24h of incubation.

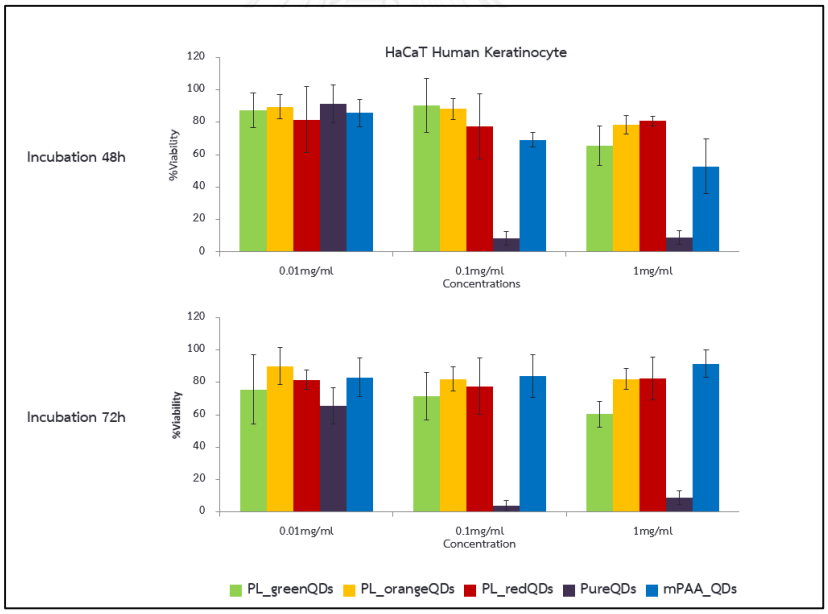

Figure 4.19: The percentages of cell viability of the PLs-coated CdSe-ZnS QDs in milliQ in different sizes compared with the original TOPO-CdSe-ZnS QDs in milliQ and the mPAA-coated green CdSe-ZnS QDs in milliQ incubated with HaCaT human keratinocytes for 48h and 72h.

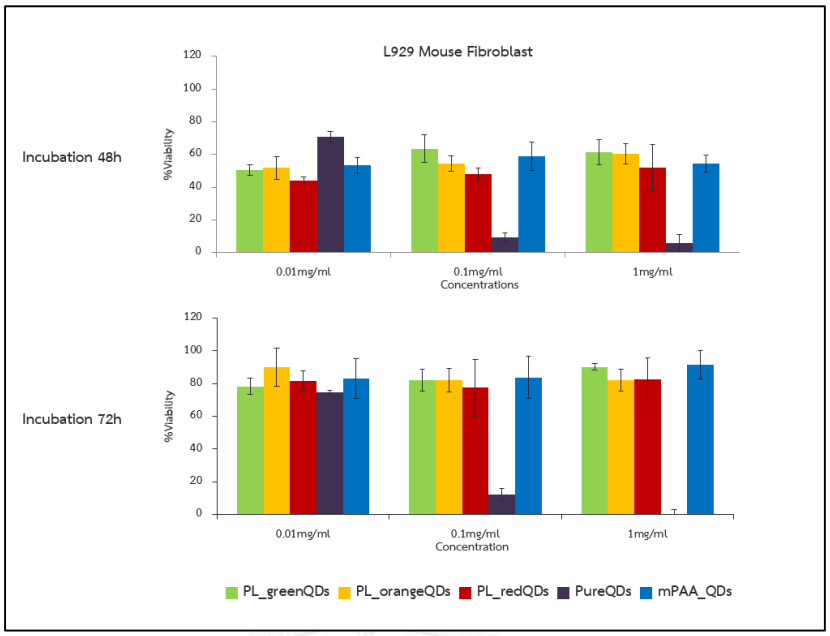

Figure 4.20: The percentages of cell viability of the PLs-coated CdSe-ZnS QDs in milliQ in different sizes compared with the original TOPO-CdSe-ZnS QDs in milliQ and the mPAA-coated green CdSe-ZnS QDs in milliQ incubated with L929 mouse fibroblast for 48h and 72h.

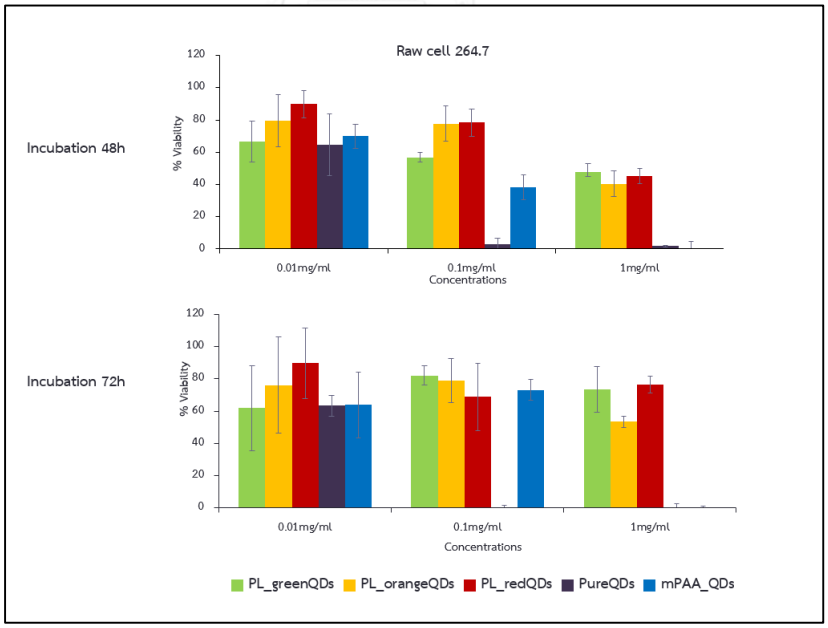

Figure 4.21: The percentages of cell viability of the PLs-coated CdSe-ZnS QDs in milliQ in different sizes compared with the original TOPO-CdSe-ZnS QDs in milliQ and the mPAA-coated green CdSe-ZnS QDs in milliQ incubated with raw cell for 48h and 72h.

In Figure 4.19 and 4.20, when both HaCaT human keratinocyte and L929 mouse fibroblast were exposed to the different concentrations of the PLs-coated with three sizes CdSe-ZnS QDs at 48h and 72h of incubation, the cell viability of the PLs-coated with three sizes of CdSe-ZnS QDs were increased to 80% at all concentrations, whereas the cell viability of the original TOPO-CdSe-ZnS QDs were dramatically decreased at high concentration of 1mg/mL and 0.1mg/mL. However, the cell viability of the mPAA-coated green CdSe-ZnS QDs were not different significantly with the PLs-coated green CdSe-ZnS QDs at the same concentrations for 48h and 72h of incubation.

In Figure 4.21, when 264.7 raw cell was exposed to the different concentrations of the PLs-coated with three sizes CdSe-ZnS QDs at 48h incubation, the percentage of cell viability of the PLs-coated with three sizes CdSe-ZnS QDs were approximately 40%-60% at all concentrations, whereas the percentage of cell viability of the original TOPO-CdSe-ZnS QDs were dramatically decreased at high concentration of 1mg/mL and 0.1mg/ml. With exposure to the mPAA-coated green CdSe-ZnS QDs, slightly reduced the cell viability when compared with the PLs-coated CdSe-ZnS green QDs at a concentration of 1mg/mL, but exposure to the mPAA-coated green CdSe-ZnS QDs showed significantly different the cell viability at high concentration of 0.1mg/mL and 0.01mg/mL.

In Figure 4.21, when 264.7 raw cell was exposed to the different concentrations of the PLs-coated with three sizes CdSe-ZnS QDs for 72h incubation, the cell viability of the PLs-coated with three sizes CdSe-ZnS QDs were approximately 60%-80% at all concentrations. , whereas the cell viability of the original TOPO-CdSe-ZnS QDs were dramatically decreased at high concentration of 1mg/mL and 0.1mg/mL. With exposure to the mPAA-coated green CdSe-ZnS QDs, dramatically decreased the cell viability when compared with the original TOPO-CdSe-ZnS QDs at high concentration of 1mg/mL.

The results indicated that coating of PLs-coated on the three sizes of CdSe-ZnS QDs were higher the cell viability than the original TOPO-CdSe-ZnS QDs at high concentrations most likely because the aqueous PLs-QDs could reduce the surface degradation and decrease cytotoxicity[62], and the prepared TOPO-CdSe-ZnS QDs were poorly dispersed in aqueous media and aggregated[63]. Moreover, the synthetic

polymer mPAA-coated CdSe-ZnS QDs showed no difference the cell viability when compared the PLs-coated CdSe-ZnS QDs in green QDs at low concentration. Thus, the camellia phospholipids as natural polymers could substitute for the synthetic polymers into QDs modification. In conclusion, the cytotoxicity of CdSe-ZnS QDs were reduced when modified with camellia phospholipids and were applied in biological applications such as target cell image for dental materials testing[64] and fluorescent probes for human skin metabolism studying.[65] The cytotoxicity of CdSe-ZnS QDs were depended on varieties of biological parameters and experiment conditions such as types of cells, types of ligands coating, incubation time, particle concentrations, etc.[66]

4.9 Cytokine inductions

The cytokine secretion after the cells was exposed to the original TOPO-CdSe-ZnS QDs, the PLs-coated CdSe-ZnS QDs of different sizes and the synthesized polymer mPAA-coated CdSe-ZnS QDs in supernatants were measured using enzyme-linked immunosorbent assay (ELISA). In the experiments, we measured the production of TNF-α, IL-6 and IL-1β cytokines using ELISA MAX™ standard set.

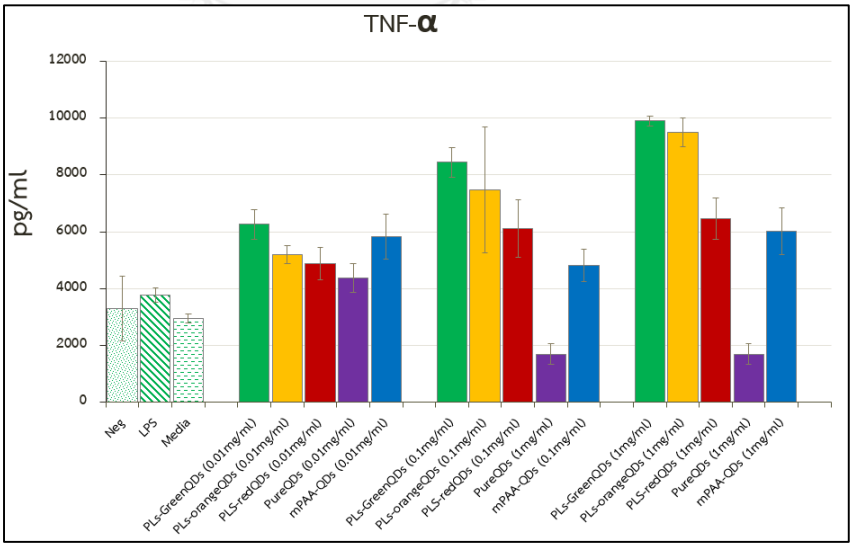

Figure 4.22: The levels of TNF-α production in supernatants of the original TOPO-CdSe-ZnS QDs, the PLs-coated CdSe-ZnS QDs of different sizes and the synthesized polymer mPAA-coated CdSe-ZnS QDs after 24 h incubation in 264.7 raw cell.

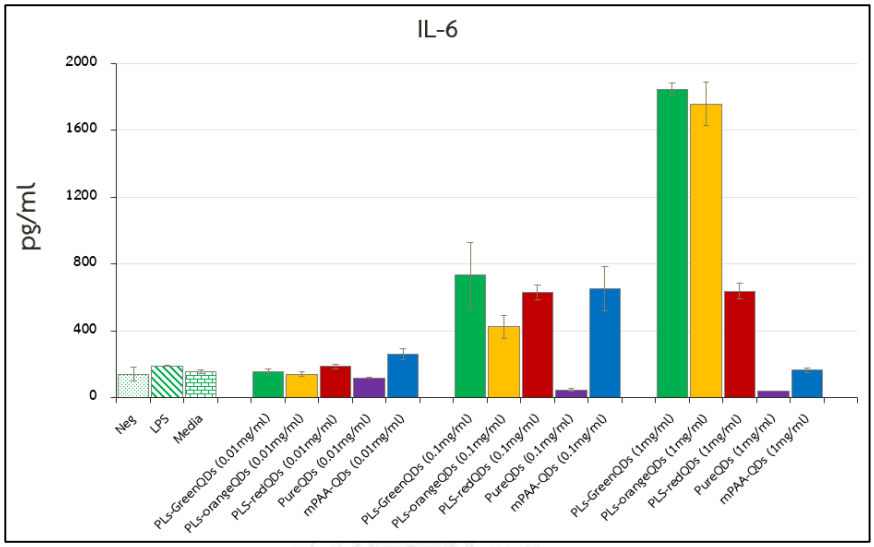

Figure 4.23: The levels of IL-6 production in supernatants of the original TOPO-CdSe-ZnS QDs, the PLs-coated CdSe-ZnS QDs of different sizes and the synthesized polymer mPAA-coated CdSe-ZnS QDs after 24 h incubation in 264.7 raw cell.

The original TOPO-CdSe-ZnS QDs, the PLs-coated CdSe-ZnS QDs of different sizes and the mPAA-coated CdSe-ZnS QDs showed the induction of TNF-α and IL-6 release, but IL-1 β were not detected after 24 h incubation in 264.7 raw cell as shown in Figures 4.22 and 4.23. The data for IL-1β detection were shown in Appendix C. The PLs-coated CdSe-ZnS QDs of three sizes slightly increased the levels of TNF-α and IL-6 secretion depending on concentrations. In contrast, the original TOPO-CdSe-ZnS QDs exhibited only a small level of TNF-α secretion at concentrations of 0.1 mg/ml and 0.01 mg/ml. Besides, when incubated with the mPAA-coated CdSe-ZnS, the level of TNF-α secretion was detected as about 5,000-6,000 pg/mL and the level of IL-6 secretion at about 200-700 pg/mL.

The results indicated that the original TOPO-CdSe-ZnS QDs induced low level of TNF-α and IL-6 secretion, while the coating of PLs-coated on the three sizes of CdSe-ZnS QDs and the mPAA-coated CdSe-ZnS QDs produced the high level of TNF-

α and IL-6 because the original TOPO-CdSe-ZnS QDs suddenly caused mortality in 264.7 raw cell at high concentration (Figure 4.18). Moreover, in our studies in IL-1β, which is a cytokine marker for identify a pyronecrosis and pyroptosis as typical cell death[67], were not detected. Therefore, the pyronecrosis and pyroptosis could not be cytotoxic mechanism in our findings.

In summary, this findings indicated that post-exposed TOPO-CdSe-ZnS QDs and modified QDs with camellia phospholipids could be effective in stimulation of immune cell and immune functions.[68]

CHAPTER V
CONCLUSIONS

The camellia phospholipids have been extracted from extra virgin of camellia oil with 85% phosphoric acid at 70°c for 30 min. The camellia phospholipids were characterized the functional groups by Fourier transforms infrared spectrometer (FT-IR). The results showed the main functional groups of phospholipids included the C-H stretching (2849 cm^{-1} and 2919.13 cm^{-1}), the C=O group (1739.46 cm^{-1}), the C-H bending (1454.66 cm^{-1}), the peaks of PO_2 (989.62 cm^{-1}) and P-O-C (1085.52 cm^{-1}). The structures of camellia phospholipids were characterized by proton nuclear magnetic resonance spectroscopy (^{1}H-NMR). The structures of camellia phospholipids were similar to the corresponding triglyceride. The phosphorus-containing species of phospholipids were analyzed by 31-Phosphorus nuclear magnetic resonance spectroscopy (^{31}P-NMR). The results showed that the camellia phospholipids were mainly phosphatidylcholine and lysophosphatidylethanolamine.

The original TOPO-CdSe-ZnS QDs have been successfully synthesized by hot injection into high boiling point of solvent and surfactant mixture resulting in QDs with three sizes, which are green QDs, orange QDs and red QDs. The original TOPO-CdSe-ZnS green QDs, the original TOPO-CdSe-ZnS orange QDs, and the original TOPO-CdSe-ZnS red QDs exhibited high quantum yield of 33.44 %, 24.29 % and 33.36 % in hexane, respectively. From TEM images, particle diameters were 2.67 nm for green QDs, 3.34 nm for orange QDs and 4.48 nm for red QDs with the highest emission wavelength at 560, 578, and 628 nm, respectively.

After modification with camellia phospholipids, the PLs-coated green CdSe-ZnS QDs, the PLs-coated orange CdSe-ZnS QDs, and the PLs-coated red CdSe-ZnS QDs were dissolved in 1 M Tris pH 10, and exhibited moderately fluorescent intensity. The quantum yield of the PLs-coated green CdSe-ZnS QDs, the PLs-coated orange CdSe-ZnS QDs, and the PLs-coated red CdSe-ZnS QDs were 2.84 %, 1.30 % and 2.43 % with the maximum emission wavelength at 566, 585, and 631 nm, respectively. From TEM images, particle sizes were 2.67 nm for PLs-coated green CdSe-ZnS QDs, 3.34 nm for

the PLs-coated orange CdSe-ZnS QDs and 4.48 nm for the PLs-coated red CdSe-ZnS QDs. The original TOPO-CdSe-ZnS QDs were successful modified with the camellia phospholipids and become dispersible in various aqueous media. The PLs-coated QDs in aqueous media retained the absorption spectra, decreased in fluorescent signals and sizes, and unchanged in shapes. The PLs-coated-QDs were dispersible and stable in aqueous media when compared with the original TOPO-QDs.

For colloidal stability, the PLs-coated with smallest CdSe-ZnS QDs was stable in basic aqueous media such as 1M Tris pH 10 for more 2 months because the PLs coated with smallest QDs are unchanged in the emission wavelength, maintained strongly fluorescent intensity and non-aggregation. However, for biological applications, the QDs should be dispersible in aqueous media at neutral pH. For experiments, the PLs-coated green CdSe-ZnS QDs in 0.01 M PBS pH 7.4 were stable about 2 weeks, and suitably used for applications within limited time after preparation.

For cytotoxicity study, the PLs-coated on the three sizes of CdSe-ZnS QDs showed higher the cell viability than the original TOPO-CdSe-ZnS QDs at high concentration for 1mg/mL. Furthermore, the cell viability of the synthetic polymer mPAA-coated CdSe-ZnS QDs were not different when compared with the cell viability of the PLs-coated CdSe-ZnS QDs in green QDs at low concentration of 0.01mg/mL. Thus, the camellia phospholipids as natural polymers could potentially substitute for the synthetic polymers QDs modification. Besides, the modification of camellia phospholipids into CdSe-ZnS QDs have also shown to reduce the QDs toxicity.

For cytokine detections, the original TOPO-CdSe-ZnS QDs, the PLs-coated CdSe-ZnS QDs of different sizes and the synthesized polymer mPAA-coated CdSe-ZnS QDs released in TNF-α, IL-6, but non-detected in IL-1β after 24 hours incubation in 264.7 raw cell. As shown in Figure 4.22 and Figure 4.23. The PLs-coated CdSe-ZnS QDs of three sizes slightly increased the levels of TNF-α and IL-6 secretion depending on concentrations. In contrast, the original TOPO-CdSe-ZnS QDs exhibited only a slightly the level of TNF-α secretion at concentrations of 0.1 mg/ml and 0.01 mg/ml. Besides,

the mPAA-coated CdSe-ZnS QDs observed the level of TNF-α secretion about 5,000-6,000 pg/ml and the level of IL-6 secretion about 200-700 pg/ml.

Thus, we could use the byproducts from plant edible oil production such as phospholipids in the preparation of water-soluble quantum dots, leading to low toxic chemicals used and QDs with low toxicity *in vitro*. In addition, we obtained water-dispersible quantum dots that were potentially useful for biological applications such as target cell imaging and fluorescent probes for metabolism studying.

REFERENCES

[1] Alagarasi, A. Introduction to nanomaterials. 2011, National Centre for Catalysis Research (NCCR) internal bulletin (Unpublished). Chennai, India.[Online]:< http://www. nccr. iitm. ac. in/2011. pdf.

[2] Fahlman, B.D. Nanomaterials. in Materials Chemistry, pp. 457-583: Springer, 2011.

[3] Tiwari, J.N., Tiwari, R.N., and Kim, K.S. Zero-dimensional, one-dimensional, two-dimensional and three-dimensional nanostructured materials for advanced electrochemical energy devices. Progress in Materials Science 57(4) (2012): 724-803.

[4] Balaguru, R.J.B. and Jeyaprakash, B. Introduction to Materials and Classification of Low Dimensional Materials. (2012).

[5] Vajtai, R. Springer handbook of nanomaterials. Springer Science & Business Media, 2013.

[6] Shou, Q., Guo, C., Yang, L., Jia, L., Liu, C., and Liu, H. Effect of pH on the single-step synthesis of gold nanoparticles using PEO–PPO–PEO triblock copolymers in aqueous media. Journal of Colloid and Interface Science 363(2) (2011): 481-489.

[7] Orbaek, A.W., McHale, M.M., and Barron, A.R. Synthesis and Characterization of Silver Nanoparticles for an Undergraduate Laboratory. Journal of Chemical Education 92(2) (2015): 339-344.

[8] Chertok, B., David, A.E., and Yang, V.C. Polyethyleneimine-modified iron oxide nanoparticles for brain tumor drug delivery using magnetic targeting and intra-carotid administration. Biomaterials 31(24) (2010): 6317-6324.

[9] injumpa, M.W. synthesis of magnetic nanoparticles and infiltration through dntine dise with mahnetic field for application in drug delivery to dental pulp. mster degree, Department of chemistry Chulalongkorn university. 2014.

[10] Anngell, J.J. Synthesis and Characterization of CdSe-ZnS core-shell quantum dots for increased quantum yield. 2011: The Faculty of the Department of Materials Engineering California Polytechnic State University San Luis Obispo. 10.

[11] Xu, L., Chen, K.J., El-Khair, H.M., Li, M.H., and Huang, X.F. Enhancement of band-edge luminescence and photo-stability in colloidal CdSe quantum dots by various surface passivation technologies. Applied Surface Science 172(1-2) (2001): 84-88.

[12] Ko, E., Lee, J., Jeon, J.-W., Lee, I., Shin, Y., and Han, I. Size tunability and optical properties of CdSe quantum dots for various growth conditions. Journal of the Korean Physical Society 62(1) (2013): 121-126.

[13] Koole, R., Groeneveld, E., Vanmaekelbergh, D., Meijerink, A., and de Mello Donegá, C. Size Effects on Semiconductor Nanoparticles. in de Mello Donegá, C. (ed.)Nanoparticles, pp. 13-51: Springer Berlin Heidelberg, 2014.

[14] Yong, K.-T., et al. Preparation of Quantum Dot/Drug Nanoparticle Formulations for Traceable Targeted Delivery and Therapy. Theranostics 2(7) (2012): 681-694.

[15] Nguyen, T.-D. and Do, T.-O. Size- and Shape-Controlled Synthesis of Monodisperse Metal Oxide and Mixed Oxide Nanocrystals. Nanocrystal. 2011.

[16] Hezinger, A.F., Tessmar, J., and Gopferich, A. Polymer coating of quantum dots--a powerful tool toward diagnostics and sensorics. Eur J Pharm Biopharm 68(1) (2008): 138-52.

[17] Ma, D.L.a.F. Soybean Phospholipids in Krezhova, P.D. (ed.)Recent Trends for Enhancing the Diversity and Quality of Soybean Products, p. 546 pages. Agricultural and Biological Sciences: InTech, Chapters published 2011.

[18] Lopes, S.C.d.A., Giuberti, C.d.S., Rocha, T.G.R., Ferreira, D.d.S., Leite, E.A., and Oliveira, M.C. Liposomes as Carriers of Anticancer Drugs. Cancer Treatment - Conventional and Innovative Approaches. 2013.

[19] McClements, D.J. and Gumus, C.E. Natural emulsifiers-biosurfactants, phospholipids, biopolymers, and colloidal particles: Molecular and physicochemical basis of functional performance. Advances in Colloid and Interface Science (2016).

[20] WU, X.-h., HUANG, Y.-f., and XIE, Z.-f. Health functions and prospective of camellia oil [J]. Food Science and Technology 8 (2005): 94-96.

[21] The Botanical Organization, M.o.N.R.a.E., Thailand BGO Plant Database, The Botanical Garden Organization. http://www.qsbg.org/database/botanic_book%20full%20option/search_detail.asp?botanic_id=2408 [Online]. 2011.

[22] foundation, C. ภัทรพัฒน์ PatPat. in *www.patpat9.com*. 2015.

[23] Deffense, E. Chemical Degumming, Edible oil processing [Online]. 2011.

[24] Srl., I.E. Edible Oil & Fat Refining [Online]. 2013.

[25] Shen, L. Biocompatible Polymer/Quantum Dots Hybrid Materials: Current Status and Future Developments. Journal of Functional Biomaterials 2(4) (2011): 355.

[26] Mattoussi, H., Palui, G., and Na, H.B. Luminescent quantum dots as platforms for probing in vitro and in vivo biological processes. Advanced Drug Delivery Reviews 64(2) (2012): 138-166.

[27] Zhang, Y. and Clapp, A. Overview of Stabilizing Ligands for Biocompatible Quantum Dot Nanocrystals. Sensors (Basel, Switzerland) 11(12) (2011): 11036-11055.

[28] Travert-Branger, N., et al. Oligomeric PEG-phospholipids for solubilization and stabilization of fluorescent nanocrystals in water. Langmuir 24(7) (2008): 3016-9.

[29] Lee, C.P. and Yen, G.C. Antioxidant activity and bioactive compounds of tea seed (*Camellia oleifera* Abel.) oil. J Agric Food Chem 54(3) (2006): 779-84.

[30] Fang, X., Yao, X., Wang, K., and Wang, Y. Effects of extraction methods on the quality of oil-tea camellia seed oil. China Oils Fats 34 (2009): 23-26.

[31] Noh, S. and Yoon, S.H. Stereospecific Positional Distribution of Fatty Acids of Camellia (Camellia japonica L.) Seed Oil. Journal of Food Science 77(10) (2012): C1055-C1057.

[32] Ceci, L.N., Constenla, D.T., and Crapiste, G.H. Oil recovery and lecithin production using water degumming sludge of crude soybean oils. Journal of the Science of Food and Agriculture 88(14) (2008): 2460-2466.

[33] Jing, W. Study on degumming technology for crude oil from pressed tea seed by phosphoric acid and hydration method. J. Anhui Agric. Sci (2008): 30.

[34] Lee, S.Y., Jung, M.Y., and Yoon, S.H. Optimization of the refining process of camellia seed oil for edible purposes. Food Science and Biotechnology 23(1) (2014): 65-73.

[35] Applewhite, T.H. Proceedings of the world conference on oilseed technology and utilization. The American Oil Chemists Society, 1993.

[36] Zhou, C., et al. A versatile method for the preparation of water-soluble amphiphilic oligomer-coated semiconductor quantum dots with high fluorescence and stability. Journal of Colloid and Interface Science 344(2) (2010): 279-285.

[37] Giri, A., Goswami, N., Lemmens, P., and Pal, S.K. Preparation of water soluble l-arginine capped CdSe/ZnS QDs and their interaction with synthetic DNA: Picosecond-resolved FRET study. Materials Research Bulletin 47(8) (2012): 1912-1918.

[38] Liu, J., et al. Single nanoparticle imaging and characterization of different phospholipid-encapsulated quantum dot micelles. Langmuir 28(28) (2012): 10602-9.

[39] Shi, Y., He, P., and Zhu, X. Photoluminescence-enhanced biocompatible quantum dots by phospholipid functionalization. Materials Research Bulletin 43(10) (2008): 2626-2635.

[40] Dubertret, B., Skourides, P., Norris, D.J., Noireaux, V., Brivanlou, A.H., and Libchaber, A. In vivo imaging of quantum dots encapsulated in phospholipid micelles. Science 298(5599) (2002): 1759-62.

[41] Hu, R., et al. PEGylated Phospholipid Micelle-Encapsulated Near-Infrared PbS Quantum Dots for in vitro and in vivo Bioimaging. Theranostics 2(7) (2012): 723-733.

[42] Liu, J., et al. Toxicity assessment of phospholipid micelle-encapsulated cadmium-based quantum dots using Kunming mice. RSC Advances 3(6) (2013): 1768-1773.

[43] Dabbousi, B., et al. (CdSe) ZnS core-shell quantum dots: synthesis and characterization of a size series of highly luminescent nanocrystallites. The Journal of Physical Chemistry B 101(46) (1997): 9463-9475.

[44] Sotirhos, N., Herslof, B., and Kenne, L. Quantitative analysis of phospholipids by 31P-NMR. J Lipid Res 27(4) (1986): 386-92.

[45] Povrozin, Y. and Terpetschnig, E. Measurement of Fluorescence Quantum Yields on ISS Instrumentation Using Vinci. 2011.

[46] Kubin, R.F. and Fletcher, A.N. Fluorescence quantum yields of some rhodamine dyes. Journal of Luminescence 27(4) (1982): 455-462.

[47] Sittampalam, G.S., et al. Cell Viability Assays. (2013).

[48] Pan, Y., et al. Size‐dependent cytotoxicity of gold nanoparticles. Small 3(11) (2007): 1941-1949.

[49] Pathakoti, K., Hwang, H.-M., Xu, H., Aguilar, Z.P., and Wang, A. In vitro cytotoxicity of CdSe/ZnS quantum dots with different surface coatings to human keratinocytes HaCaT cells. Journal of Environmental Sciences 25(1) (2013): 163-171.

[50] Haiyan, Z., Bedgood Jr, D.R., Bishop, A.G., Prenzler, P.D., and Robards, K. Endogenous biophenol, fatty acid and volatile profiles of selected oils. Food Chemistry 100(4) (2007): 1544-1551.

[51] Vlachos, N., Skopelitis, Y., Psaroudaki, M., Konstantinidou, V., Chatzilazarou, A., and Tegou, E. Applications of Fourier transform-infrared spectroscopy to edible oils. Anal Chim Acta 573-574 (2006): 459-65.

[52] Nzai, J.M. and Proctor, A. Determination of phospholipids in vegetable oil by fourier transform infrared spectroscopy. Journal of the American Oil Chemists' Society 75(10) (1998): 1281-1289.

[53] Norazlan, M., Aziz, A., and Kamal, M. Process Design In Degumming And Bleaching Of Palm Oil. (2006).

[54] Chapman, D. and Morrison, A. Physical Studies of Phospholipids IV. HIGH RESOLUTION NUCLEAR MAGNETIC RESONANCE SPECTRA OF PHOSPHOLIPIDS AND RELATED SUBSTANCES. Journal of Biological Chemistry 241(21) (1966): 5044-5052.

[55] Hatzakis, E., Koidis, A., Boskou, D., and Dais, P. Determination of Phospholipids in Olive Oil by 31P NMR Spectroscopy. Journal of Agricultural and Food Chemistry 56(15) (2008): 6232-6240.

[56] Jangle, R., Galge, R., Patil, V., and Thorat, B. Selective HPLC method development for soy phosphatidylcholine fatty acids and its mass spectrometry. Indian journal of pharmaceutical sciences 75(3) (2013): 339.

[57] Amaro, A.L. and Almeida, D.P.F. Lysophosphatidylethanolamine effects on horticultural commodities: A review. Postharvest Biology and Technology 78 (2013): 92-102.

[58] Lara, N. and Barron, A.R. P-31 NMR Spectroscopy. 1.2 (2013).

[59] Liu, Z., Liu, S., Yin, P., and He, Y. Fluorescence enhancement of CdTe/CdS quantum dots by coupling of glyphosate and its application for sensitive detection of copper ion. Anal Chim Acta 745 (2012): 78-84.

[60] Jin, T., Fujii, F., Komai, Y., Seki, J., Seiyama, A., and Yoshioka, Y. Preparation and characterization of highly fluorescent, glutathione-coated near infrared quantum dots for in vivo fluorescence imaging. International journal of molecular sciences 9(10) (2008): 2044-2061.

[61] Shaw, D.R. Dynamic Light Scattering Training Achieving reliable nano particle sizing Malvern, Editor.: http://www.atascientific.com.au.

[62] Derfus, A.M., Chan, W.C., and Bhatia, S.N. Probing the cytotoxicity of semiconductor quantum dots. Nano letters 4(1) (2004): 11-18.

[63] Uyeda, H.T., Medintz, I.L., Jaiswal, J.K., Simon, S.M., and Mattoussi, H. Synthesis of compact multidentate ligands to prepare stable hydrophilic quantum dot fluorophores. Journal of the American Chemical Society 127(11) (2005): 3870-3878.

[64] Thonemann, B., Schmalz, G., Hiller, K.A., and Schweikl, H. Responses of L929 mouse fibroblasts, primary and immortalized bovine dental papilla-derived cell lines to dental resin components. Dental Materials 18(4) (2002): 318-323.

[65] Lehmann, B. HaCaT cell line as a model system for vitamin D3 metabolism in human skin. J Invest Dermatol 108(1) (1997): 78-82.

[66] Kirchner, C., et al. Cytotoxicity of colloidal CdSe and CdSe/ZnS nanoparticles. Nano letters 5(2) (2005): 331-338.

[67] Kroemer, G., et al. Classification of cell death: recommendations of the Nomenclature Committee on Cell Death 2009. Cell death and differentiation 16(1) (2009): 3-11.

[68] Wang, X., et al. Immunotoxicity assessment of CdSe/ZnS quantum dots in macrophages, lymphocytes and BALB/c mice. J Nanobiotechnology 14 (2016): 10.

VITA

Mr. Sarawuth Phaenthong was born on August 19, 1989 in Samutsakhon Provinces, Thailang. He graduated in Bachelor Degree of Science in Biology from Chulalongkorn University in 2012. He continued his Master's Degree of Science in Program in Biotechnology, Faculty of Science, and Chulalongkorn University. He became a member of Materials Chemistry and Catalysis Research Unit under the supervision of Dr. Numpon Insin. On 6-8 November 2015, he attended the 14th Congress on Science and Technology of Thailand (STT41) conference 2015 in the title of "SURFACE MODIFICATION OF SEMICONDUCTOR NANOCRYSTALS QUANTUM DOTS WITH PLANT PHOSPHOLIPIDS" by poster presentation.

His present address is 873/4, Phahonyothin Road., Samsennai, Phayathai, Bangkok, Thailand, 10280

Email address: Sarawuth.p@hotmail.com

APPENDIX A

Determination of fatty acid compositions by Gas chromatography

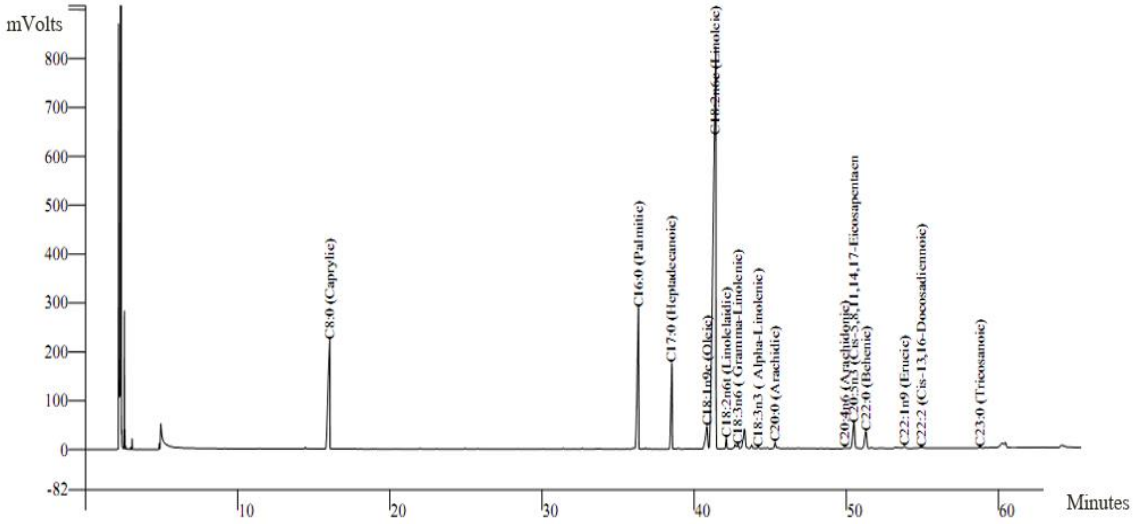

Figure A1: GC chromatogram of Fatty Acid Methyl Ester (FAME) of *Camellia oleifera* Abel oil. (Camellia oil)

APPENDIX B

Calculation of quantum yield following the equation;

$$Q = Q_R \left(\frac{m}{m_R}\right)\left(\frac{n^2}{n_R^2}\right)$$

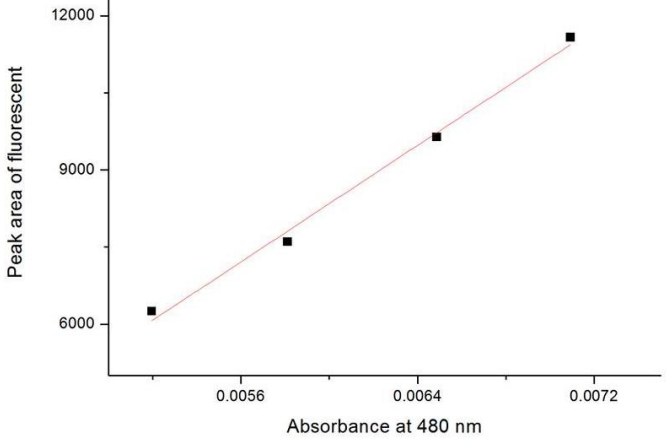

Table B1: Parameters of the linear regression of Rhodamine 6G emission

	Intercept	Slope	Adj. R-Square
Peak area of fluorescent	-8663.31657	2.83501×10^6	0.99063

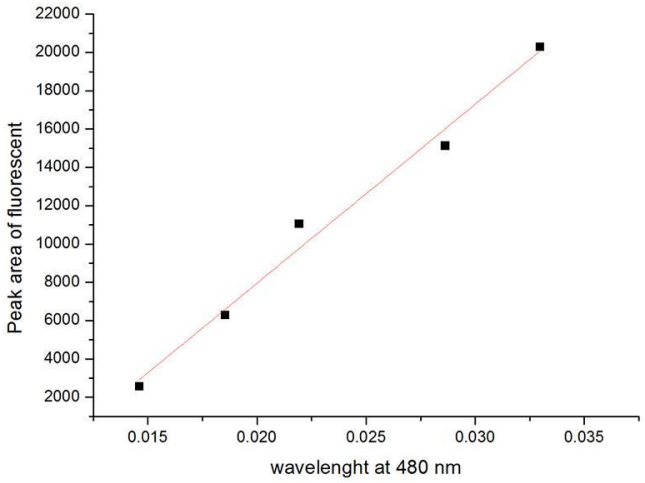

Table B2: Parameters of linear regression of the emission from the green original TOPO-CdSe-ZnS QDs in hexane

	Intercept	Slope	Adj. R-Square
Peak area of fluorescent	-10730.83501	934378.98026	0.98147

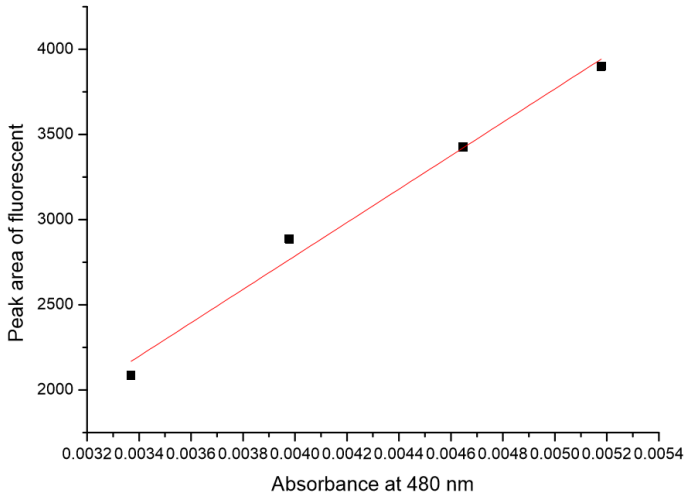

Table B4: Parameters of linear regression of the emission from the red original TOPO-CdSe-ZnS QDs in hexane

	Intercept	Slope	Adj. R-Square
Peak area of fluorescent	-1137.05269	980994.91889	0.98118

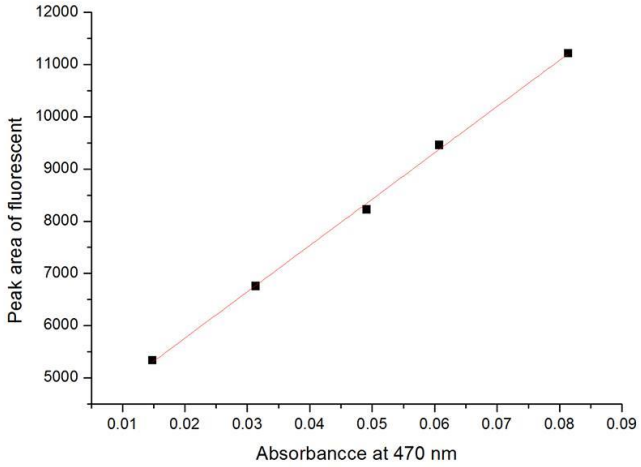

Table B5: The value of linear regression of the PLs-coated green CdSe-ZnS QDs in 1 M Tris pH 10.

	Intercept	Slope	Adj. R-Square
Peak area of fluorescent	3989.77062	88700.56996	0.9985

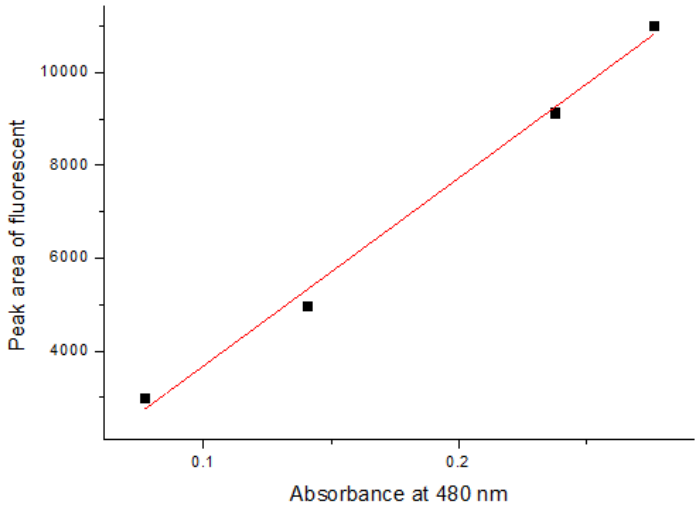

Table B6: The value of linear regression of the PLs-coated orange CdSe-ZnS QDs in 1 M Tris pH 10.

	Intercept	Slope	Adj. R-Square
Peak area of fluorescent	-369.03867	40479.89614	0.99153

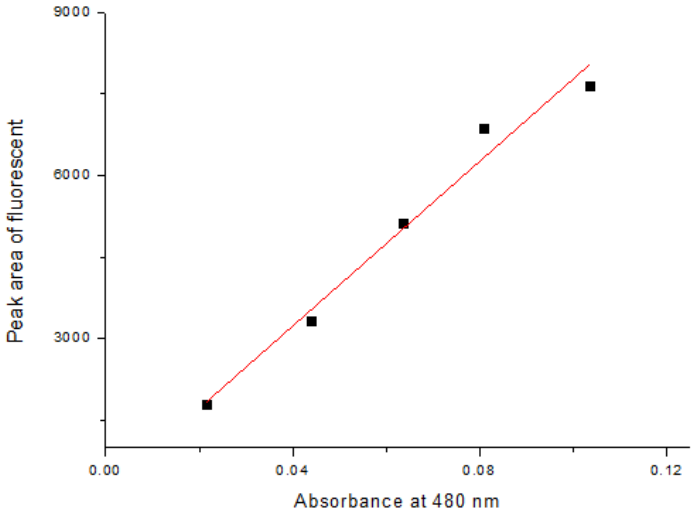

Table B7: The value of linear regression of the PLs-coated red CdSe-ZnS QDs in 1 M Tris pH 10.

	Intercept	Slope	Adj. R-Square
Peak area of fluorescent	205.70333	75742.91577	0.97085

APPENDIX C

IL-12p70-Biolegand Plate-ID: 20160622-IL-1beta

Standards

Response Formula	nominal	Adjusted	OD
S1	4000	3981.17	1.269
S2	2000	2048.91	0.889
S3	1000	922.08	0.503
S4	500	588.15	0.353
S5	250	203.54	0.163
S6	125	118.87	0.121
S7	62.5	74.81	0.1

Sample list

Sample-ID	Position	pg/ml	OD	Results
PR1	C1	62.87	0.094	
PR2	C2	<62.50	0.086	
PR3	C3	<62.50	0.049	
PR4	C4	71.58	0.098	
PR5	C5	<62.50	0.06	
PR6	C6	<62.50	0.064	
PR7	C7	<62.50	0.067	
PR8	C8	<62.50	0.066	
PR9	C9	<62.50	0.071	
PR10	C10	<62.50	0.057	
PR11	C11	<62.50	0.054	
PR12	C12	<62.50	0.036	
PR13	D1	<62.50	0.047	
PR14	D2	<62.50	0.035	
PR15	D3	<62.50	0.031	
PR16	D4	<62.50	0.035	
PR17	D5	<62.50	0.055	
PR18	D6	<62.50	0.06	
PR19	D7	<62.50	0.065	
PR20	D8	<62.50	0.051	
PR21	D9	<62.50	0.03	
PR22	D10	<62.50	0.048	
PR23	D11	<62.50	0.063	
PR24	D12	<62.50	0.069	

PR25	E1	<62.50	0.075
PR26	E2	<62.50	0.054
PR27	E3	<62.50	0.042
PR28	E4	<62.50	0.056
PR29	E5	<62.50	0.046
PR30	E6	<62.50	0.051
PR31	E7	<62.50	0.067
PR32	E8	<62.50	0.058
PR33	E9	<62.50	0.053
PR34	E10	<62.50	0.045
PR35	E11	<62.50	0.043
PR36	E12	<62.50	0.07
PR37	F1	<62.50	0.073
PR38	F2	<62.50	0.064
PR39	F3	<62.50	0.058
PR40	F4	<62.50	0.082
PR41	F5	<62.50	0.029
PR42	F6	<62.50	0.047
PR43	F7	<62.50	0.054
PR44	F8	<62.50	0.066
PR45	F9	<62.50	0.057
PR46	F10	<62.50	0.036
PR47	F11	<62.50	0.031
PR48	F12	75.89	0.1
PR49	G1	<62.50	0.063
PR50	G2	<62.50	0.066
PR51	G3	<62.50	0.042
PR52	G4	<62.50	0.045
PR53	G5	<62.50	0.035
PR54	G6	<62.50	0.064
PR55	G7	126.05	0.124
PR56	G8	250.17	0.186
PR57	G9	279.87	0.201
PR58	G10	<62.50	0.002
PR59	G11	<62.50	0.003
PR60	G12	<62.50	0.003
PR61	H1	<62.50	0.001
PR62	H2	<62.50	0.002
PR63	H3	<62.50	0.001
PR64	H4	<62.50	0.001
PR65	H5	<62.50	0.001

PR66	H6	<62.50	0.001
PR67	H7	<62.50	0
PR68	H8	<62.50	0.002
PR69	H9	<62.50	0.001
PR70	H10	<62.50	0.003
PR71	H11	<62.50	0.002
PR72	H12	<62.50	0.002

Info Controls

S1	A1 B1	0	1.269
S2	A2 B2	0	0.889
S3	A3 B3	0	0.503
S4	A4 B4	0	0.353
S5	A5 B5	0	0.163
S6	A6 B6	0	0.121
S7	A7 B7	0	0.1
S8	A8 B8	0	0.097
S9	A9 B9	0	0.131
S10	A10 B10	0	0.094
S11	A11 B11	0	0.109
S12	A12 B12	0	0.122